Table 1 Proportion of cases (percentage of cases in parentheses) containing ubiquitinated (UBQ) and TDP-43 immunoreactive inclusions in neurons of inferior olives, together with median rating values for each type of inclusion, for each patient group

Group	Proportion UBQ +ve	Median UBQ rating	0	0.5	1	2	3	4	Proportion TDP +ve	Median TDP rating	0	0.5	1	2	3	4
FTLD	37/48 (77)	1	11	8	10	10	8	1	13/48 (27)	0	35	5	4	2	1	1
FTLD-TDP	26/32 (81)	3	6	7	5	5	8	1	13/32 (40)	0	19	5	4	2	1	1
FTLD-U type 1	8/9 (89)	1	1	3	1	2	2	0	1/9 (18)	0	8	1	0	0	0	0
FTLD-U type 2	6/10 (60)	2	4	3	1	0	2	0	2/10 (20)	0	8	2	0	0	0	0
FTLD-U type 3	12/13 (91)	3	1	1	3	3	4	1	10/13 (78)	1	3	2	4	2	1	1
FTLD-tau	10/15 (67)	1	5	0	5	5	0	0	0/15 (0)	0	15	0	0	0	0	0
FTLD-Picks	4/8 (50)	1	4	0	3	1	0	0	0/8 (0)	0	8	0	0	0	0	0
FTLD-*MAPT*	6/7 (86)	2	1	0	2	4	0	0	0/7 (0)	0	7	0	0	0	0	0
FTLD-DLDH	1/1 (100)	0	0	1	0	0	0	0	0/1 (0)	0	0	0	0	0	0	0
MND	10/11 (91)	1	1	5	2	2	1	0	2/11 (18)	0	9	0	2	0	0	0
AD	5/5 (100)	2	0	1	1	2	1	0	1/5 (20)	0	0	1	0	0	0	0
DLB	5/7 (71)	2	2	0	1	2	1	1	0/7 (0)	0	7	0	0	0	0	0
HD	1/3 (33)	0	2	1	0	0	0	0	0/3 (0)	0	3	0	0	0	0	0
PD	13/19 (68)	1	6	3	5	4	1	0	0/19 (0)	0	19	0	0	0	0	0
PSP	11/11 (100)	1	0	1	5	5	0	0	0/11 (0)	0	11	0	0	0	0	0
MSA	2/6 (33)	0	4	0	2	0	0	0	0/6 (0)	0	6	0	0	0	0	0
Control	14/14 (100)	1	0	0	8	3	3	0	0/14 (0)	0	14	0	0	0	0	0

Also shown is the number of cases falling into each rating category for each patient group

FTLD frontotemporal lobar degeneration, *MND* motor neurone disease, *AD* Alzheimer's disease, *DLB* dementia with Lewy bodies, *HD* Huntington's disease, *PD* Parkinson's disease, *PSP* progressive supranuclear palsy, *MSA* multisystem atrophy

cells) in only a single FTLD-U type 1 case, and in two type 2 cases. In FTLD-tau, UBQ-ir NCI were present in 4/8 (50%) sporadic FTLD cases with Pick bodies and 6/7 (80%) cases FTLD with *MAPT* mutations. In all cases of FTLD-tau, and in the DLDH case, NCI were always of the conglomerated type. Elsewhere, UBQ-ir NCI were also seen in 10/11 (91%) patients with MND, these being of the spicular type in 2 patients but of the conglomerated type in the other 8 patients. UBQ-ir NCI were also present in 5/5 (100%) patients with AD (1 with spicular NCI and 4 with conglomerated NCI), 5/7 (71%) patients with DLB, 13/19 (68%) patients with PD, 11/11(100%) patients with PSP, 2/6 (33%) patients with MSA, 1/3 (33%) patients with HD, and in 14/14 (100%) normal elderly control subjects. In all these, latter groups of patients NCI were always of a conglomerated type.

The proportion of patients with UBQ-ir inclusions was broadly similar in all patient groups (Table 1), though the small sample sizes of some groups prevented formal statistical comparisons across all the groups. Within FTLD group alone, there was no difference in proportion of patients with UBQ-ir inclusions between those with FTLD-TDP and those with FTLD-tau ($\chi^2 = 1.21$, $P = 0.270$), or between the three different FTLD-U histological subtypes ($\chi^2 = 4.35$, $P = 0.113$). The density of UBQ-ir inclusions (i.e., the median number of UBQ-ir inclusions per section) differed significantly ($F_{7,115} = 2.24$; $P = 0.036$) across the patient groups, though post hoc testing did not reveal any significant differences between any two of the patient groups. Although the density of UBQ-ir inclusions in FTLD-TDP did not differ from than that in FTLD-tau ($F_{1,45} = 1.65$; $P = 0.205$), there was a tendency for this to differ within the FTLD-U histological subtypes ($F_{2,29} = 2.54$; $P = 0.096$), with highest densities being seen in cases with type 3 histology and lowest in those with type 2 histology (Table 1). The density of UBQ-ir inclusions also tended to be greater ($P = 0.099$) in those FTLD-U type 3 cases with *PGRN* mutations compared to those without *PGRN* mutations.

TDP-43 immunostaining

In TDP-43 immunostaining (TDP-43-ir), using the phospho-independepent TDP-43 antibody, fewer or no NCI were seen compared to UBQ-ir stained sections. However, when present, these TDP-43-ir NCI always had a compacted or solid appearance, being rounded or spicular similar in appearance (Fig. 1e), similar to those seen on UBQ-ir (Fig. 1b, c). No TDP-43-ir NCI with a conglomerated appearance was ever seen. Occasionally, skein-like

NCI were also seen. Frequently, neurones contained a fine granular TDP-43 deposition, either diffusely throughout the perikaryon or more peripherally around the cell margin. Occasional neurones containing NCI appeared to be devoid of intracellular organelles and nucleus, and cells undergoing neuronophagia with clustered microglia and extracellular NCI were sometimes observed (Fig. 1f). There was variable physiological nuclear staining within neurones of the ION, though glial cell nuclei and cytoplasm remained unstained in all cases.

Similar results were obtained with the polyclonal phospho-dependent TDP-43 antibody, ps409/410–2, with the exception that the normal diffuse pattern of nuclear staining was not present with this antibody. All patients and sections displaying TDP-43 pathological changes with the phospho-independent antibody were also immunoreactive with the pS409/410 antibody, with no additional patients/sections displaying TDP-43-ir.

TDP-43-ir inclusions were seen in 13/48 (27%) FTLD cases, being present in 13/32 (40%) FTLD-TDP cases (including 1/4 FTLD-MND cases), but were not seen in any of the 8 sporadic FTLD cases with Pick bodies or any of the 7 cases with FTLD with *MAPT* mutation, or in the single DLDH case. TDP-43-ir inclusions similar to those in FTLD-TDP were seen in 2/11 (18%) patients with MND and 1/5 (20%) patients with AD, but were absent in all patients with DLB or HD. With regards to FTLD-U histological type, TDP-43-ir NCI were present in 1/9 (11%) cases with type 1 histology, 2/10 (20%) cases with type 2 histology, but were seen in 10/13 (78%) cases with type 3 histology.

Within the FTLD group, the proportion of patients with TDP-43-ir inclusions was significantly greater in cases with FTLD-TDP compared to those with FTLD-tau (Fisher's exact test $P = 0.004$), and the proportion of patients with TDP-43-ir inclusions was significantly greater in cases of FTLD-U with type 3 histology compared with other FTLD-U histological subtypes ($\chi^2 = 12.22$, $P = 0.002$). The density of TDP-43-ir inclusions (i.e., the median number of TDP-43-ir inclusions per section) did not differ significantly between FTLD overall and the other patient groups ($F_{7,115} = 1.68$; $P = 0.120$), though the density of TDP-43-ir inclusions in FTLD-TDP was significantly greater than that in FTLD-tau ($F_{1,45} = 5.20$; $P = 0.027$). Moreover, the density of TDP-43-ir inclusions within the different FTLD-U histological subtypes differed significantly ($F_{2,29} = 4.59$; $P = 0.019$), with highest densities in cases with type 3 histology and lowest in those with type 1 histology. The density of TDP-43-ir inclusions in those FTLD-U type 3 cases with *PGRN* mutations was greater (Fisher's exact test $P = 0.05$) than that in those cases without *PGRN* mutations.

Comparison of density of UBQ-ir and TDP-43-ir NCI

The density of NCI within each case, as determined by both UBQ and TDP-43 immunostaining, was compared on a group basis using Wilcoxon signed ranks test. The density of UBQ-ir NCI was significantly greater than that of TDP-43-ir NCI for FTLD-U histology types 1 ($P = 0.007$), 2 ($P = 0.017$) and 3 ($P = 0.048$), FTLD with *MAPT* mutations ($P = 0.023$), MND ($P = 0.038$), AD ($P = 0.043$), DLB ($P = 0.042$), PD ($P = 0.000$), PSP ($P = 0.000$), MSA ($P = 0.000$), and in the normally aged group ($P = 0.000$) and tended to be greater ($P = 0.059$) in FTLD with Pick bodies; there was no significant difference ($P = 0.317$) between the density of UBQ-ir and TDP-43-ir NCI in HD.

Relationship to age

There was a highly significant correlation ($r_s = 0.394$; $P < 0.001$) between rating for UBQ-ir inclusions and age at death (where known) for those 108 subjects (i.e., patients and normal controls) without TDP-43-ir inclusions: patients with TDP-43-ir inclusions were excluded from this analysis since the presence of such inclusions would have contributed partially or wholly to the overall UBQ-ir inclusion score. Nonetheless, a similar relationship with age was seen amongst those remaining 16 patients with TDP-43-ir inclusions ($r_s = 0.581$; $P = 0.018$).

Other immunostaining

In all cases with UBQ-ir NCI, similar appearing NCI were also seen in p62 immunostaining (Fig. 1). While the spicular or skein-like UBQ-ir NCI were as strongly immunoreactive with p62 antibody (Fig. 1g) as those seen in UBQ (Fig. 1b) or TDP-43 (Fig. 1e) immunostaining, the conglomerated type (Fig. 1h) were sometimes, but not always, as strongly immunoreactive with p62 antibody as with UBQ immunostaining (Fig. 1a). None of the type of inclusion was detected with antibodies to phosphorylated tau, neurofilament, α-synuclein or α-internexin proteins.

Double immunostaining and confocal microscopy

Double labelling immunohistochemistry showed that most of the spicular and rounded TDP-43-ir inclusions within ION were also UBQ-ir (Fig. 2a), though occasional spicular TDP-43-ir NCI were seen that were not UBQ-ir (Fig. 2b). Sometimes, within the same cell, there were two spicular NCI, one containing both TDP-43 and UBQ proteins, and one with only TDP-43-ir apparently not being ubiquitinated (Fig. 2c). On other occasions, spicular NCI showed parts of the inclusion to be TDP-43-ir and parts

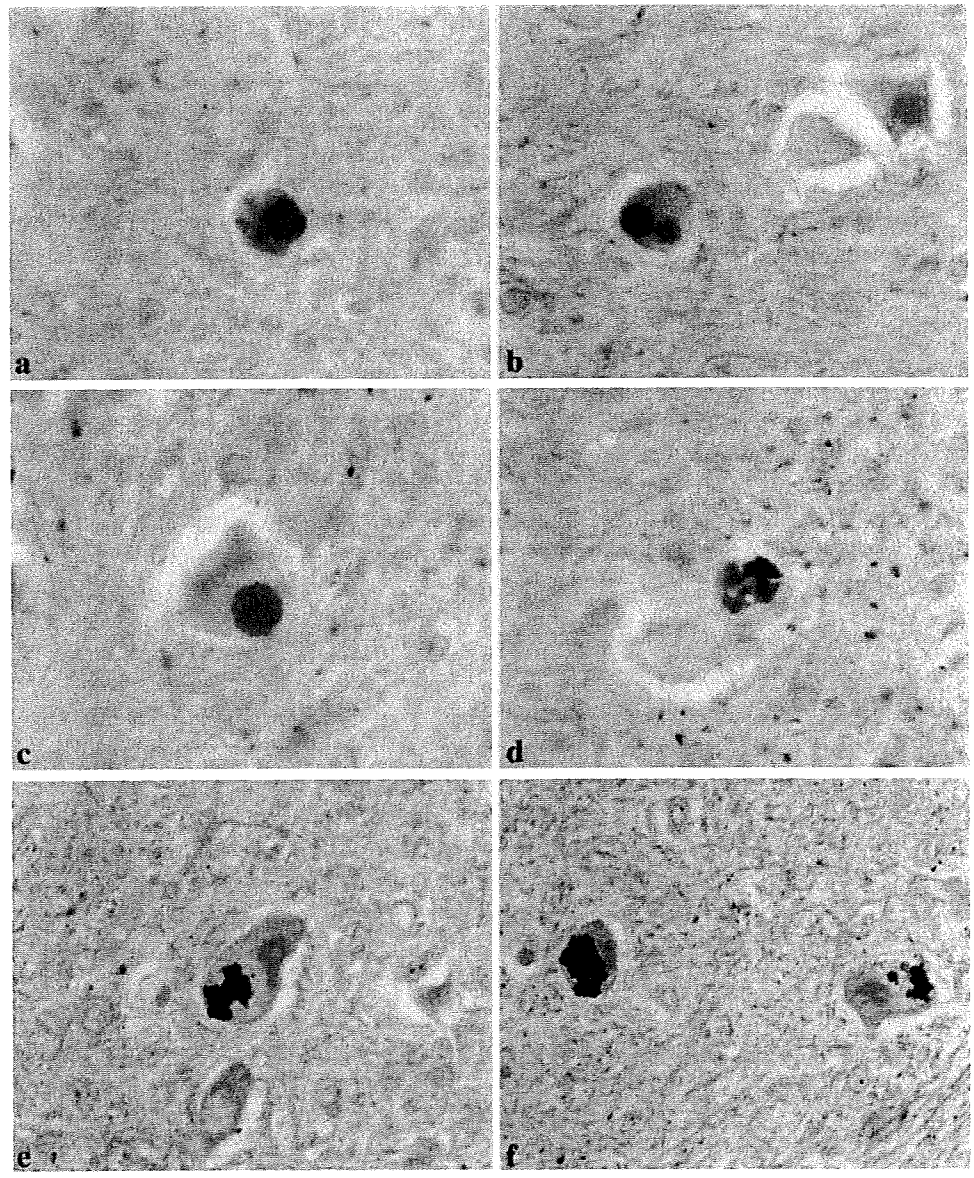

Fig. 2 Double immunolabelling of neuronal cytoplasmic inclusions (NCI) in neurones of the inferior olivary nucleus. Most of the spicular and rounded TDP-43-ir NCI (*brown*) are also UBQ-ir (*purple*) (**a, b**), though occasional TDP-43-ir NCI are not UBQ-ir (**b, c**), sometimes even within the same cell where the other NCI is both TDP-43-ir and UBQ-ir (**c**). On other occasions, parts of NCI are TDP-43-ir and parts UBQ-ir (**d**). The conglomerated, UBQ-ir NCI are not TDP-43-ir (**e, f**). Microscope objective magnification ×40

that were UBQ-ir were seen (Fig. 2d). Conversely, the conglomerated, UBQ-ir type of NCI were never TDP-43-ir (Fig. 2e, f).

Confocal microscopy confirmed that the spicular and rounded, UBQ-ir NCI (Fig. 3a) were also TDP-43-ir (Fig. 3b), and that in some instances, the two proteins appeared to be co-localised (Fig. 3c). The conglomerated UBQ-ir NCI did not contain TDP-43 protein (not shown).

Nuclear immunostaining

TDP-43 is a DNA binding protein and therefore most cases showed variable degrees of physiological nuclear immunostaining with the phospho-independent TDP-43 antibody, this ranging from very strong to weak or absent in each of the diagnostic groups. Nonetheless, it was notable that in FTLD-TDP, MND and AD groups, olivary neurones with TDP-43-ir NCI showed no TDP-43 nuclear staining (Fig. 1e) (see also [10]), whereas neurones without NCI showed a degree of nuclear staining comparable with that seen in neurones in other brain stem regions (e.g., those in vestibular or hypoglossal nuclei) where UBQ or TDP-43 NCI were never seen. Nuclear TDP-43-ir was not diminished in neurones of ION showing conglomerated TDP-43-negative, UBQ-ir NCI compared to cells without such UBQ-ir inclusions.

Discussion

The presence of ubiquitinated inclusions in the ION has been commented on in some early studies [12, 14, 17],

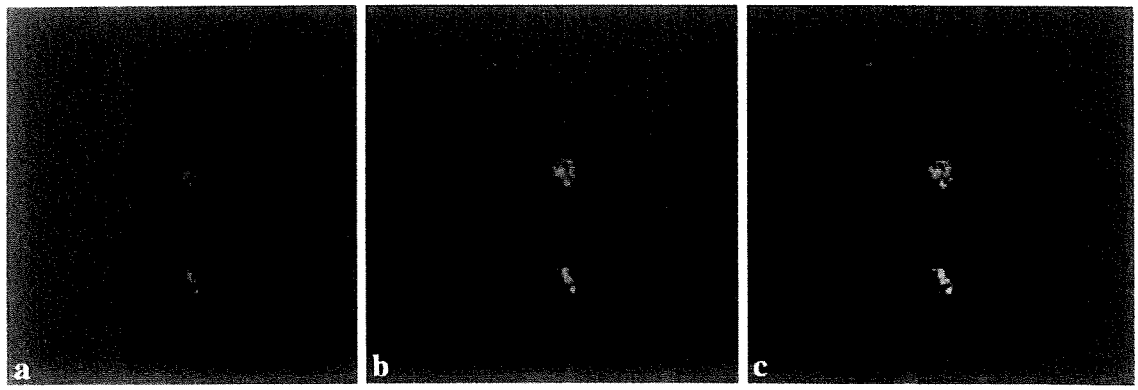

Fig. 3 Confocal microscopy shows that the spicular and rounded, UBQ-ir NCI are also TDP-43-ir, and that the two proteins are co-localised (a UBQ green, b TDP-43 red, c merge). Microscope objective magnification ×100

though these observations were made largely on normally aged persons and in some patients with AD. Likewise, some previous studies on FTLD-TDP and FTLD-MND using UBQ immunohistochemistry [25] or TDP-43 immunohistochemistry [10] have alluded to the presence of ubiquitinated, or TDP-43-containing, NCI within the inferior and superior olivary nuclei, however, there has only been one previous systematic study of these structures in FTLD [11]. In this, TDP-43-ir NCI, similar in range of morphologies to those described here, were present in 79% of (51) cases of FTLD-TDP, 50% of (4) cases of FTLD-MND and 50% of (11) cases of MND alone. Unfortunately, these authors did not further classify the presence of TDP-43-ir NCI in ION according to FTLD-U histological subtype, or in relationship to genetic cause. Consequently, the specificity of NCI to patients with FTLD-TDP and MND is unknown, and their relationship to clinical and histological phenotype, and relevance to disease symptomatology, remains to be clarified. In the present report, investigating patients with neurodegenerative diseases such as FTLD, MND, AD, DLB, PD, PSP, MSA or HD, and normally aged individuals, we have noted NCI to be widely present in the inferior olives in many patients with different neurodegenerative disorders and in normal elderly persons. Two types of (mutually exclusive) NCI were seen.

The first type was UBQ/p62 and TDP-43 immunoreactive and had a solid, rounded, spicular or skein like appearance. This type of inclusion was mostly present in patients with FTLD-TDP, especially those with FTLD-U type 3 histology [8, 29] and *PGRN* mutation. Such inclusions were less common in FTLD-U type 3 cases without *PGRN* mutations, being similar in frequency to those in FTLD-U cases with types 1 and 2 histology [8, 29]. This kind of inclusion was also seen in a few patients with MND and occasionally ones with AD, but was not seen in FTLD-tau, in the single patient with DLDH, in patients with DLB, PD, PSP or HD, or in normal elderly individuals. The presence of TDP-43-ir inclusions in the ION in FTLD-TDP and MND patients may therefore represent an 'extension' of the pathological process to involve this particular brain region along with cerebral cortex, hippocampus, striatum, brain stem and spinal cord. TDP-43 pathology has been noted to occur in the temporal cortex and hippocampus in about 25% patients with AD [1], and the (occasional) appearance of such NCI in ION in AD may reflect this wider cerebral cortical involvement. Indeed, the single AD case showing TDP-43-ir NCI in ION also displayed widespread cerebral cortical and hippocampal TDP-43 pathological changes. Consistent with our previous findings within the cerebral cortex [10], we were unable to demonstrate TDP-43-ir NCI within ION in a variety in patients with FTLD-tau, including sporadic cases with Pick bodies and familial cases associated with *MAPT* exon 10 +13 or +16 mutations.

The pathophysiological relevance of these TDP-43-ir NCI in ION remains unclear. TDP-43 is a 43 kDa protein composed of 414 amino acids which may function as a transcription repressor or an initiator of exon skipping in the alternative splicing of mRNA [2, 40]. As a transcription factor, a physiological presence of TDP-43 within nerve cell nuclei would be anticipated. However, as reported in cerebral cortical and hippocampal neurones [2, 40], there was a complete lack of nuclear TDP-43 immunostaining in cells of inferior olives in which TDP-43-ir NCI were present. It has been suggested [40] that TDP-43 inclusions may stem from a translocation of TDP-43 protein from the nucleus to the cytoplasm, though it is also possible that TDP-43 is "prevented" by hyperphosphorylation [2, 40] from crossing the nuclear membrane, thereby aggregating within the cytoplasm with loss of nuclear regulatory function [10].

The second type of NCI in ION was UBQ/p62 immunoreactive but TDP-43 negative and had a clumped or cluster-like appearance, resembling a collection of small

granules or larger globules. This type of inclusion appears to be similar to that which has been described previously in haematoxylin–eosin and UBQ immunostaining [12, 14, 17]. The target protein within these UBQ/p62 immunoreactive, TDP-43 negative, NCI remains elusive, though present and previous data [17] indicate this is unlikely to be tau, neurofilament, α-synuclein or α-internexin—proteins identified within other pathological structures, such as neurofibrillary tangles, Lewy bodies or intermediate filament inclusion bodies, within these groups of disorders. In contrast to TDP-43-ir NCI, these TDP-43 negative NCI were not associated with loss of physiological nuclear TDP-43 binding.

This type of NCI occurred with broadly equivalent frequency and density across all diagnostic groups, and within each of the FTLD histological subtypes. There did not appear to be an obvious relationship between the presence and density of these UBQ/p62 immunoreactive, TDP-43 negative NCI and age at onset, or duration, of illness in any of the diagnostic groups, or across all groups collectively, though there was a strong correlation with age at death. These findings are consistent with previous observations showing that the frequency of this kind of NCI increases within the ION with increasing age, such that after the age of 70 years, all individuals display this kind of pathological change within neurones of ION [11, 17]. Indeed, in the present study, all 20 normal individuals, who were all aged between 58 and 93 years showed such NCI. Moreover, such NCI were more common within those older patient groups with neurodegenerative disease (i.e., PD, DLB, PSP groups) than the younger patient groups (e.g., HD, MND, FTLD), being present at frequencies similar to those seen in the normal group of individuals of that age. Hence, the presence of these NCI in ION is more likely to represent some manifestation of 'the ageing process' within this particular cell type, rather than being related to (any particular) neurodegenerative disease per se. Despite, being UBQ/p62 immunoreactive, such NCI are not immunostained by anti-proteasome antibodies [14], suggesting that whatever the target protein within them might be, it is not degraded through the proteasome or, if it is normally proteolysed through this route, this fails to happen in later life and the target protein becomes 'assimilated' into these NCI and accumulated within the cell body. There have been various studies looking at changes in number of nerve cells in the human ION both in ageing [19, 35, 36, 42] and in AD [19]. While some studies have concluded that there was no cell loss with ageing [19, 35, 36], others have reported a modest cell loss both in ageing [42] and in AD [19]. Because lipofuscin accumulation is one of the more obvious pathological changes in cells of ION with ageing [31, 32] and in AD [30], there has been interest in whether this might be responsible for, or at least associated with, cell loss. Although increases in lipofuscin pigment have been associated with loss of ribosomal RNA [30] and Golgi apparatus [4] from ION, it cannot be concluded that lipofuscin accumulation per se is directly responsible for any cell loss from ION that might occur in later life or AD. The lack of neurofibrillary changes in this brain region in both ageing and in AD means that neurodegenerative pathways involving tau protein are unlikely causes, and lack of tau proteins within the UBQ-ir NCI would be consistent with this, though it is appreciated that NFT can sometimes be present within cells of ION in PSP. Nonetheless, the extracellular deposits of UBQ/p62 protein, resembling once internalised NCI, might indeed bear witness to a loss of neurones from this region with age or neurodegeneration. Identification of the target protein within such NCI might therefore provide clues to the pathogenesis of cell loss from ION in ageing and neurodegeneration.

Acknowledgments Dr. Bandopadhyaya is funded by the Parkinson's Disease Society of UK. The work of the Manchester Brain Bank is supported by the Alzheimers Research Trust and Alzheimers Society through the Brains for Dementia Research Initiative. We thank The UK Parkinson's Disease Society Tissue Bank for providing tissue samples.

References

1. Amador-Ortiz C, Lin W-L, Ahmed Z, Personett D, Davies P, Duara R, Graff-Radford NR, Hutton ML, Dickson DW (2007) TDP-43 immunoreactivity in hippocampal sclerosis and Alzheimer's disease. Ann Neurol 61:435–445
2. Arai T, Hasegawa M, Akiyama H, Ikeda K, Nonaka T, Mori H, Mann D, Tsuchiya K, Yoshida M, Hashizume Y, Oda T (2006) TDP-43 is a component of ubiquitin-positive tau-negative inclusions in frontotemporal lobar degeneration and amyotrophic lateral sclerosis. Biochem Biophys Res Commun 351:602–611
3. Baker M, Mackenzie IRA, Pickering-Brown SM, Gass J, Rademakers R, Lindholm C, Snowden J, Adamson J, Sadovnick AD, Rollinson S, Cannon A, Dwosh E, Neary D, Melquist S, Richardson A, Dickson D, Eriksen J, Robinson T, Zehr C, Dickey CA, Crook R, McGowan E, Mann D, Boeve B, Feldman H, Hutton M (2006) Mutations in *Progranulin* cause tau-negative frontotemporal dementia linked to chromosome 17. Nature 442:916–919
4. Barden H (1970) Relationship of Golgi thiamine pyrophosphatase and lysosomal acid phosphatase to neuromelanin and lipofuscin in cerebral neurones of ageing rhesus monkeys. J Neuropathol Exp Neurol 29:225–240
5. Boeve BF, Baker M, Dickson DW, Parisi JE, Giannini C, Jsephs KA, Hutton M, Pickering-Brown SM, Rademakers R, Tang-Wai D, Jack CR, Kantarci K, Shiung MM, Golde T, Smith GE, Geda YE, Knopman DS, Petersen RC (2006) Frontotemporal dementia and Parkinsonism associated with the IVS1 + 1G → A mutation in progranulin: a clinicopathologic study. Brain 129:3103–3114
6. Brooks B, Miller R, Swash M, Munsat T (2000) El Escorial revisited: revised criteria for the diagnosis of amyotrophic lateral sclerosis. Amyotroph Lateral Scler Other Motor Neuron Disord 1:293–299
7. Brun A, Englund E, Gustafson L, Passant U, Mann DMA, Neary D, Snowden JS (1994) Clinical, neuropsychological and

neuropathological criteria for fronto-temporal dementia. J Neurol Neurosurg Psychiatry 57:416–418
8. Cairns NJ, Bigio EH, Mackenzie IRA, Neumann M, Lee VM, Hatanpaa KJ, White CL III, Schneider JA, Grinberg LT, Halliday G, Duyckaerts C, Lowe JS, Holm IE, Tolnay M, Okamoto K, Yokoo H, Murayama S, Woulfe J, Munoz DG, Dickson DW, Ince PG, Trojanowski JQ, Mann DMA (2007) Neuropathologic diagnostic and nosologic criteria for frontotemporal lobar degeneration: consensus of the Consortium for Frontotemporal Lobar Degeneration. Acta Neuropathol 114:5–22
9. Cruts M, Gijselinck I, van der Zee J, Engelborghs S, Wils H, Pirici D, Rademakers R, Vandenberghe R, Dermaut B, Martin J-J, van Duijn C, Peeters K, Sciot R, Santens P, De Pooter T, Mattheijssens M, Van den Broeck M, Cujit I, Vennekens K, De Deyn PP, Kumar-Singh S, Van Broeckhoven C (2006) Null mutations in progranulin cause ubiquitin-positive frontotemporal dementia linked to chromosome 17q21. Nature 442:920–924
10. Davidson Y, Kelley T, Mackenzie IR, Pickering-Brown SM, Du Plessis D, Neary D, Snowden JS, Mann DMA (2007) Ubiquitinated pathological lesions in frontotemporal lobar degeneration contain the TAR DNA-binding protein, TDP-43. Acta Neuropathol 113:521–533
11. Dickson DW, Josephs KA, Amador-Ortiz C (2007) TDP-43 in the differential diagnosis of motor neuron disorders. Acta Neuropathol 114:71–79
12. Dickson DW, Wertin A, Kress Y, Ksiezak-Reding H, Yen S-H (1990) Ubiquitin immunoreactive structures in normal human brains. Lab Invest 63:87–99
13. Forman MS, Farmer J, Johnson JK, Clark CM, Arnold SE, Coslett HB, Chatterjee A, Hurtig HI, Karlawish JH, Rosen HJ, Van Deerlin V, M-Y LeeV, Miller BL, Trojanowski JQ, Grossman M (2006) Frontotemporal dementia: clinicopathological correlations. Ann Neurol 59:952–962
14. Ii K, Ito H, Tanaka K, Hirano A (1997) Immunocytochemical co-localization of the proteasome in ubiquitinated structures in neurodegenerative diseases and the elderly. J Neuropathol Exp Neurol 56:125–131
15. Josephs KA, Holton JL, Rossor MN, Godbolt AK, Osawa T, Strand K, Khan N, Al-Sarraj S, Revesz T (2004) Frontotemporal lobar degeneration and ubiquitin immunohistochemistry. Neuropathol Appl Neurobiol 30:369–373
16. Josephs KA, Petersen RC, Knopman DS, Boeve BF, Whitwell JL, Duffy JR, Parisi JE, Dickson DW (2006) Clinicopathologic analysis of frontotemporal and corticobasal degenerations and PSP. Neurology 66:41–48
17. Kato S, Hirano A, Suenaga T, Yen S-H (1990) Ubiquitinated eosinophilic granules in the inferior olivary nucleus. Neuropathol Appl Neurobiol 16:135–139
18. Katsuse O, Dickson DW (2005) Ubiquitin immunohistochemistry of frontotemporal lobar degeneration differentiates cases with and without motor neurone disease. Alzheimer Dis Assoc Disord 19(suppl 1):S37–S43
19. Lasn H, Winblad B, Bogdanovic N (2001) The number of neurons in the inferior olivary nucleus in Alzheimer's disease and normal ageing: a stereological study using the optical fractionator. J Alzheimer's Disease 3:159–168
20. Leigh PN, Anderton BH, Dodson A, Gallo J-M, Swash M, Power DM (1988) Ubiquitin deposits in anterior horn cells in motor neurone disease. Neurosci Lett 93:197–203
21. Lipton AM, White CL III, Bigio EH (2004) Frontotemporal lobar degeneration with motor neuron disease-type inclusions predominates in 76 cases of frontotemporal degeneration. Acta Neuropathol 108:379–385
22. Litvan I, Hauw JJ, Bartko JJ, Lantos PL, Daniel SE, Horoupian DS, McKee A, Dickson D, Bancher C, Tabaton M, Jellinger K, Anderson DW (1996) Validity and reliability of the preliminary NINDS neuropathologic criteria for progressive supranuclear palsy and related disorders. J Neuropath Exp Neurol 55:97–105
23. Lowe JS, Lennox G, Jefferson D, Morrell K, McQuire D, Gray T, Landon M, Doherty FJ, Mayer RJ (1988) A filamentous inclusion body within anterior horn neurones in motor neurone disease detected by immunocytochemical localisation of ubiquitin. Neurosci Lett 94:203–210
24. Mackenzie IRA, Feldman H (2003) The relationship between extramotor ubiquitin-immunoreactive neuronal inclusions and dementia in motor neurone disease. Acta Neuropathol 105:98–102
25. Mackenzie IRA, Feldman HH (2005) Ubiquitin immunohistochemistry suggests classic Motor Neuron Disease, Motor Neuron Disease with dementia and Frontotemporal dementia of the Motor Neuron Disease type represent a clinicopathologic spectrum. J Neuropathol Exp Neurol 64:730–739
26. Mackenzie IRA, Baborie A, Pickering-Brown SM, Du Plessis D, Jaros E, Perry RH, Neary D, Snowden JS, Mann DMA (2006) Heterogeneity of ubiquitin pathology in frontotemporal lobar degeneration. Acta Neuropathol 112:539–549
27. Mackenzie IRA, Baker M, Pickering-Brown S, Hsiung G-Y, Lindholm C, Dwosh E, Gass J, Cannon A, Rademakers R, Hutton M, Feldman H (2006) The neuropathology of frontotemporal lobar degeneration caused by mutations in the *progranulin* gene. Brain 129:3081–3090
28. Mackenzie IRA, Shi J, Shaw CL, Du Pleassis D, Neary D, Snowden D, Mann DMA (2006) dementia lacking distinctive histology (DLDH) revisited. Acta Neuropathol 112:551–559
29. Mackenzie IRA, Neumann M, Bigio E, Cairns NJ, Alafuzoff I, Krill J, Kovacs GG, Ghetti B, Halliday G, Holm IR, Ince PG, Kamphourst W, Revesz T, Rozemuller AJM, Kumar-Singh S, Akiyama H, Baborie A, Spina S, Dickson DW, Trojanowski JQ, Mann DMA (2009) Nomenclature for neuropathologic subtypes of frontotemporal lobar degeneration: consensus recommendations. Acta Neuropathol 117:15–18
30. Mann DMA, Sinclair KGA (1978) The quantitative assessment of lipofuscin pigment, cytoplasmic RNA and nucleolar volume in senile dementia. Neuropathol Appl Neurobiol 4:129–135
31. Mann DMA, Yates PO (1974) Ageing in the human nervous system. I The lipofuscin content of nerve cells. Brain 97:481–488
32. Mann DMA, Yates PO, Stamp JE (1978) Relationship of lipofuscin pigment to ageing in the human nervous system. J Neurol Sci 35:83–93
33. McKeith IG, Galasko D, Kosaka K, Perry EK, Dickson DW, Hansen LA, Salmon DP, Lowe J, Mirra SS, Byrne EJ, Lennox G, Quinn NP, Edwardson JA, Ince PG, Bergeron C, Burns A, Miller BL, Lovestone S, Collerton D, Jansen EN, Ballard C, de Vos RA, Wilcock GK, Jellinger KA, Perry RH (1996) Consensus guidelines for the clinical and pathological diagnosis of dementia with Lewy bodies (DLB): report of the consortium on DLB international workshop. Neurology 47:1113–1124
34. Mirra SS, Heyman A, McKeel D, Sumi SM, Crain BJ, Brownlee LM, Vogel FS, Hughes JP, Belle G, Berg L (1991) The consortium to establish a registry for Alzheimer's disease. Part II. Standardization of the neuropathologic assessment of Alzheimer's disease. Neurology 41:479–486
35. Moatamed F (1966) Cell frequencies in the human inferior olivary nuclear complex. J Comp Neurol 128:109–116
36. Monagle RD, Brody H (1974) Effects of age upon the main nucleus of the inferior olive in humans. J Comp Neurol 155: 61–66
37. Mott RT, Dickson DW, Trojanowski JQ, Zhukareva V, Lee VM, Forman M, Van Deerlin V, Ervin JF, Wang DS, Schmechel DE, Hulette CM (2005) Neuropathologic, biochemical, and molecular characterization of the frontotemporal dementias. J Neuropathol Exp Neurol 64:420–428

38. Mukherjee O, Pastor P, Cairns NJ, Chakraverty S, Kauwe JSK, Shears S, Behrens MJ, Budde J, Hinrichs AL, Norton J, Levich D, Taylor-Reinwald L, Gitcho M, Tu P-H, Grinberg LT, Liscic RM, Armendariz J, Morris JC, Goate AM (2006) HDDD2 is a familial frontotemporal lobar degeneration with ubiquitin-positive, tau-negative inclusions caused by a missense mutation in the signal peptide of progranulin. Ann Neurol 60:314–322
39. Neary D, Snowden JS, Gustafson L, Passant U, Stuss D, Black S, Freedman M, Kertesz A, Robert PH, Albert M, Boone K, Miller BL, Cummings J, Benson DF (1998) Frontotemporal lobar degeneration: A consensus on clinical diagnostic criteria. Neurology 51:1546–1554
40. Neumann M, Sampathu DM, Kwong LK, Truax AC, Micsenyi MC, Chou TT, Bruce J, Schuk T, Grossman M, Clark CM, McCluskey LF, Miller BL, Masliah E, Mackenzie IR, Feldman H, Feiden W, Kretzschmar H, Trojanowski JQ, Lee VM (2006) Ubiquitinated TDP-43 in frontotemporal lobar degeneration and amyotrophic lateral sclerosis. Science 314:130–133
41. Pickering-Brown SM, Baker M, Gass J, Boeve BF, Loy CT, Brooks WS, Mackenzie IR, Martins RN, Kwok JB, Halliday GM, Kril JJ, Schofield PR, Mann DM, Hutton M (2006) Mutations in progranulin explain atypical phenotypes with variants in MAPT. Brain 129:3124–3126
42. Sandoz P, Meier-Ruge W (1977) Age-related loss of nerve cells from the human inferior olives and unchanged volume of its grey matter. IRCS Med Sci 5:376
43. Shi J, Shaw CL, Richardson AMT, Bailey K, Tian J, Varma AR, Neary D, Snowden JS, Mann DMA (2005) Histopathological changes underlying frontotemporal lobar degeneration with clinicopathological correlation. Acta Neuropathol 110:501–512
44. Snowden JS, Pickering-Brown SM, Mackenzie IR, Richardson AMT, Varma A, Neary D, Mann DMA (2006) Progranulin gene mutations associated with frontotemporal dementia and progressive aphasia. Brain 129:3091–3102
45. Taniguchi S, McDonagh AM, Pickering-Brown SM, Umeda Y, Iwatsubo T, Hasegawa M, Mann DMA (2004) The neuropathology of frontotemporal lobar degeneration with respect to the cytological and biochemical characteristics of tau protein. Neuropathol Appl Neurobiol 30:1–18
46. Trojanowski JQ, Revesz T, Neuropathology Working Group on MS (2007) Proposed neuropathological criteria for the post mortem diagnosis of multiple system atrophy. Neuropathol Appl Neurobiol 33:615–620
47. Woulfe J, Kertesz A, Munoz D (2001) Frontotemporal dementia with ubiquitinated cytoplasmic and intranuclear inclusions. Acta Neuropathol 102:94–102

FEBS Letters 583 (2009) 2419–2424

FEBS Letters

journal homepage: www.FEBSLetters.org

Methylene blue and dimebon inhibit aggregation of TDP-43 in cellular models

Makiko Yamashita [a,1], Takashi Nonaka [a,1], Tetsuaki Arai [b], Fuyuki Kametani [a], Vladimir L. Buchman [c], Natalia Ninkina [c,d], Sergey O. Bachurin [d], Haruhiko Akiyama [b], Michel Goedert [e], Masato Hasegawa [a,*]

[a] Department of Molecular Neurobiology, Tokyo Institute of Psychiatry, Tokyo Metropolitan Organization for Medical Reearch, 2-1-8 Kamikitazawa, Setagaya-ku, Tokyo 156-8585, Japan
[b] Department of Psychogeriatrics, Tokyo Institute of Psychiatry, Tokyo Metropolitan Organization for Medical Research, 2-1-8 Kamikitazawa, Setagaya-ku, Tokyo 156-8585, Ja
[c] School of Biosciences, Cardiff University, Cardiff CF10 3US, UK
[d] Institute of Physiologically Active Compounds, RAS, Chernogolovka 142432, Russian Federation
[e] MRC Laboratory of Molecular Biology, Hills Road, Cambridge CB2 0QH, UK

ARTICLE INFO

Article history:
Received 18 May 2009
Revised 10 June 2009
Accepted 22 June 2009
Available online 26 June 2009

Edited by Jesus Avila

Keywords:
Tau
Alpha-synuclein
Inhibitor
Alzheimer
ALS
FTLD

ABSTRACT

Amyotrophic lateral sclerosis (ALS) and frontotemporal lobar degeneration with ubiquitin inclusions (FTLD-U) are major neurodegenerative diseases with TDP-43 pathology. Here we inv gated the effects of methylene blue (MB) and dimebon, two compounds that have been reporte be beneficial in phase II clinical trials of Alzheimer's disease (AD), on the formation of TDP-43 ag gates in SH-SY5Y cells. Following treatment with 0.05 μM MB or 5 μM dimebon, the number of T 43 aggregates was reduced by 50% and 45%, respectively. The combined use of MB and dime resulted in a 80% reduction in the number. These findings were confirmed by immunoblot anal The results indicate that MB and dimebon may be useful for the treatment of ALS, FTLD-U and o TDP-43 proteinopathies.

1. Introduction

Amyotrophic lateral sclerosis (ALS) is a neurodegenerative disease that is characterized by progressive weakness and muscle wasting, and for which no effective therapies exist. Frontotemporal lobar degeneration (FTLD) is the second most common form of dementia after Alzheimer's disease (AD) in the population below the age of 65 years. In many cases with these disorders, ubiquitin (Ub)-positive, tau-negative intracytoplasmic inclusions form in nerve cells and glial cells. TAR DNA binding protein of 43 kDa (TDP-43) is the major component of these inclusions [1–3]. Biochemical and histological analyses demonstrated that TDP-43 accumulates in brain and spinal cord in a hyperphosphorylated and fibrillar form [4]. Furthermore, missense mutations in the TDP-43 gene have been identified in familial cases of ALS and ALS with FTLD-U [5–9]. Together, these findings indicate that dysfunction of TDP-43 is central to the etiology and pathogenesis of ALS and FTLD-U. In addition, TDP-43 has also been found to accumulate in other neurodegenerative disorders, including AD, dementia with Lewy bodies [10], Parkinsonism-dementia complex of Guam [11], argyrophilic grain disease [12], Huntington's dis [13], Perry syndrome [14] and familial British dementia [15].

Inhibition of the aggregation of TDP-43 and promotion o clearance are considered to be major therapeutic avenues for and FTLD-U. As for other neurodegenerative diseases, current t include antibodies, synthetic peptides, molecular chaperones chemical compounds. Of the latter, methylene blue (MB) dimebon have recently been reported to have significant benefi effects in phase II clinical trials of AD [16,17]. MB is a phenot zine compound that has been used for treating methemoglob mia [18,19], inhibiting nitric oxide synthase [20], reducing nC [21], enhancing β-oxydation in mitochondria [22], inhibitin noradrenaline re-uptake [23] and enhancing brain mitochond cytochrome oxidase activity [24,25]. It has also been shown to hibit AD-like Aβ and tau aggregation in vitro [26,27]. Dimebon non-selective anti-histaminergic compound that was in clinical for many years before more selective agents became available [It has been reported to inhibit butyrylcholinesterase, acetylcho esterase, NMDA receptors, voltage-gated calcium channels, ad ergic receptors, histamine H1 receptors, histamine H2 recep and serotonin receptors, as well as to stabilize glutamate-indu Ca^{2+} signals [29–31]. The effects of dimebon on pathological tein aggregation have not been studied in detail, but recently demonstrated that chronic administration of this drug redu

* Corresponding author. Fax: +81 3 3329 8035.
E-mail address: masato@prit.go.jp (M. Hasegawa).
[1] These authors contributed equally to this work.

0014-5793/$36.00
doi:10.1016/j.febslet.2009.06.042

the number of nerve cell deposits in a mouse model of synucleinopathy [32].

Here we investigated whether MB and dimebon can reduce the formation of TDP-43 inclusions in SH-SY5Y cellular models. Significantly, the treatment of cells with each compound and their combined application inhibited the formation of TDP-43 aggregates, suggesting that MB and dimebon may be effective for the treatment of ALS and FTLD-U.

2. Materials and methods

2.1. Antibodies

A polyclonal anti-TDP-43 antibody (anti-TDP-43) was purchased from ProteinTech Group Inc. (10782-1-AP, Chicago, USA). A polyclonal antibody specific for phosphorylated TDP-43 (anti-pS409/410) (available from Cosmo Bio Co., Tokyo, Japan) [4] and an anti-Ub antibody (MAB1510, Chemicon, Billerica, USA) were used for the evaluation of pathological forms of TDP-43.

2.2. TDP-43 cellular models and addition of compounds

To investigate the effects of MB and dimebon on the formation of TDP-43 aggregates, we used two cellular models of TDP-43 proteinopathy. The first consists of SH-SY5Y cells expressing mutant TDP-43 that lacks both the nuclear localization signal (NLS) and residues 187–192 (ΔNLS&187-192). In these cells, round structures positive for both anti-pS409/410 and anti-Ub are observed [33]. The second model consists of SH-SY5Y cells expressing an aggregation-prone TDP-43 C-terminal fragment (residues 162–

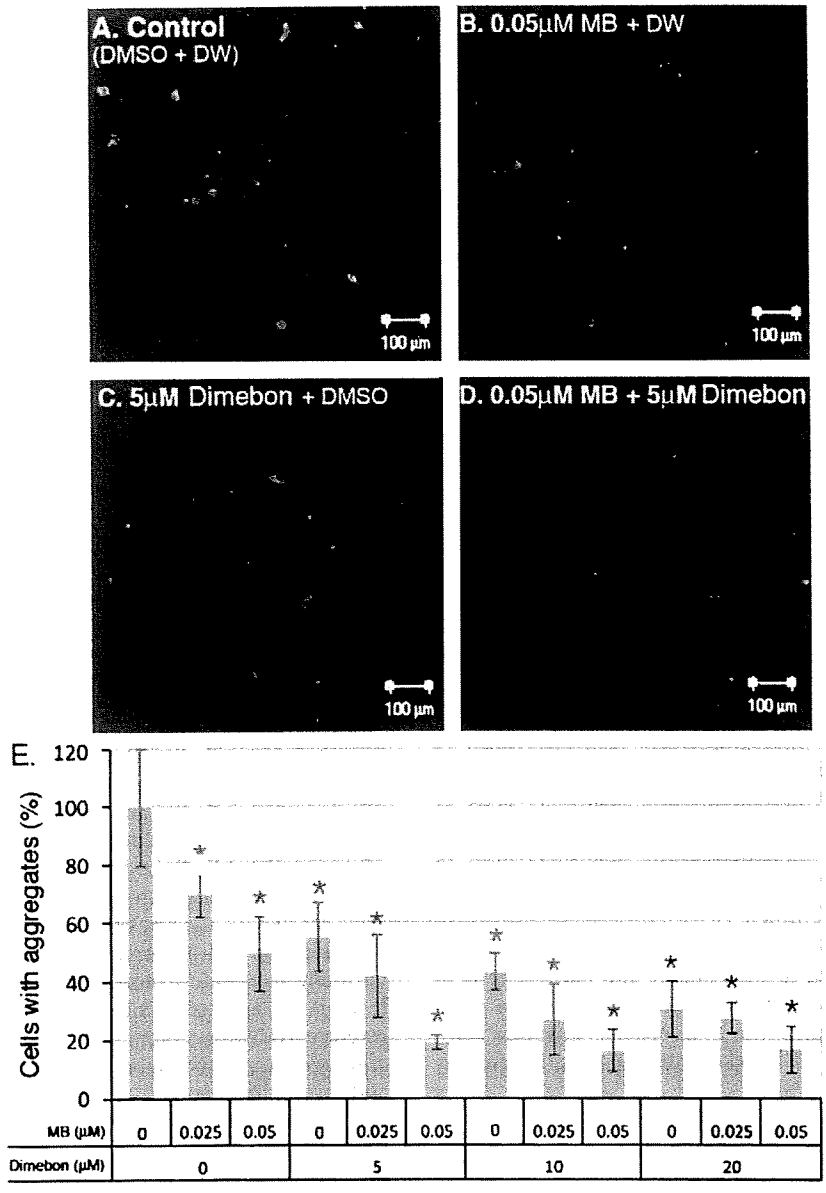

Fig. 1. Immunohistochemical analysis of the effects of methylene blue (MB) and dimebon on the aggregation of TDP-43 in SH-SY5Y cells expressing TDP-43 (ΔNLS&187-192). TDP-43 inclusions were stained with anti-pS409/410 antibody and detected with Alexa Fluor 488-labeled secondary antibody. Representative confocal images from cells treated with control (DMSO + DW) (A), 0.05 μM MB + DW (B), 5 μM dimebon + DMSO (C) and 0.05 μM MB + 5 μM dimebon (D) are shown. (E) Quantitation of cells with TDP-43 aggregates. The number of cells with intracellular TDP-43 aggregates was counted and expressed as the percentage of cells with aggregates in the absence of compound (taken as 100%). Fluorescence intensity within an area of approximately 800 μm × 800 μm was assessed by confocal microscopy. The intensity of Alexa Fluor 488 was calculated as the ratio of that of TO-PRO-3. At least 8 areas per sample were measured (n = 8–16). Data are means ± S.E.M. $^*P < 0.01$ by Student's t test.

414) as a green fluorescent protein (GFP)-fusion [34,35]. Its expression also results in the formation of anti-pS409/410- and anti-Ub-positive inclusions. Six hours after transfection, the cells were treated with MB (Sigma–Aldrich, St. Louis, USA) dissolved in dimethyl sulfoxide (DMSO), dimebon dissolved in sterile distilled water (DW) or MB + dimebon and cultured for 3 days. As controls, cells were treated with either DMSO or DW, or both of them for 3 days.

2.3. Immunohistochemical analysis

SH-SY5Y cells were grown on coverslips and transfected as described [33]. After incubation for the indicated times, the cells were fixed with 4% paraformaldehyde and stained with anti-phosphorylated TDP-43 antibody pS409/410 or anti-Ub, followed by Alexa Fluor 488- or Alexa Fluor 568-labeled IgG (Invitrogen, Carlsbad, USA). After washing, the cells were further incubated with TO-PRO-3 (Invitrogen, Carlsbad, USA) to stain nuclear DNA. To quantify the cells with TDP-43 aggregates, the laser power (at 488 nm for detection of Alexa Fluor 488 and GFP) was adjusted, so that only aggregates were detected as described [34]. Total intensity of fluorescence detected at the threshold laser power and that of TO-PRO-3 fluorescence, the latter corresponding to the total number of cells in a given field (approximately 800 μm × 800 μm), were measured with LSM5 Pascal v 4.0 software (Carl Zeiss), and the ratio of cells with inclusions calculated.

2.4. Immunoblot analysis

Tris saline (TS)-soluble, Triton X-100 (TX)-soluble and Sarkosyl (Sar)-soluble fractions, as well as the final pellet, were prepared,

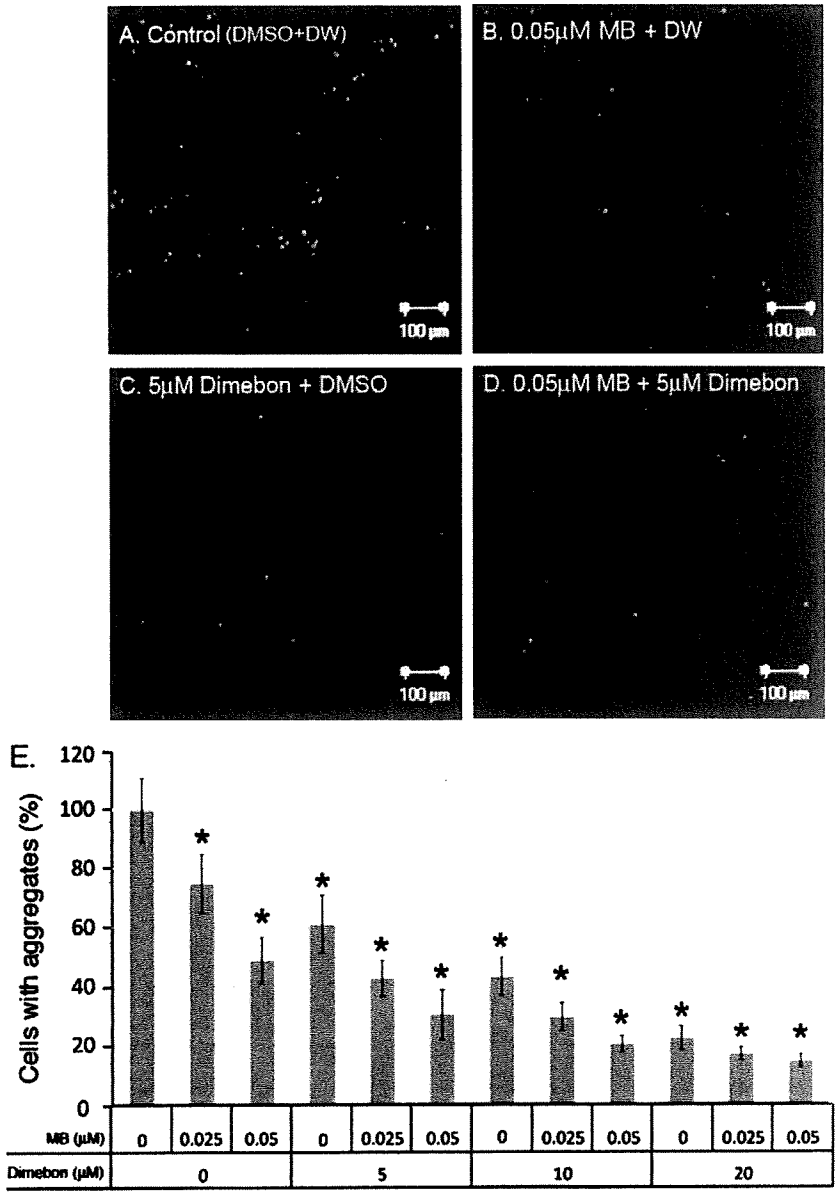

Fig. 2. Immunohistochemical analysis of the effects of methylene blue (MB) and dimebon on the aggregation of TDP-43 in SH-SY5Y cells expressing TDP-43 C-terminal fragment (162–414) as GFP fusion protein. TDP-43 inclusions were detected by fluorescence of GFP, when the laser power was adjusted. Representative confocal images from cells treated with control (DMSO + DW) (A), 0.05 μM MB + DW (B), 5 μM dimebon + DMSO (C) and 0.05 μM MB + 5 μM dimebon (D) are shown. (E) Quantitation of cells with TDP-43 aggregates. The intensity of fluorescence of GFP was calculated as the ratio of that of TOPRO-3. At least 8 areas per sample were measured ($n = 8$–16). Data are means ± S.E.M. $^{*}P < 0.01$ by Student's t test.

run on SDS–PAGE and immunoblotted with anti-TDP-43 and anti-pS409/410 antibodies, as described [33].

3. Results

3.1. Effects of MB and dimebon on the formation of TDP-43 inclusions

We first investigated the cytotoxicity of MB and dimebon. SH-SY5Y cells were treated with different concentrations of each compound, cultured for 1 day, followed by growth measurements. No toxic effects were detected with dimebon at concentrations of 1–60 μM, whereas a significant decrease in the number of cells was observed with MB at concentrations greater than 0.1 μM. Cells transfected with TDP-43 (ΔNLS&187-192) formed round intracellular inclusion-like structures that were positive with both anti-pS409/410 and anti-Ub antibodies, as reported previously [33] (Fig. 1A). When the cells were treated for 3 days with MB, dimebon or MB + dimebon, the number of TDP-43 inclusions was reduced (Fig. 1B–D). Compared to controls, we observed a 50% reduction in the number of inclusions with 0.05 μM MB, a 45% reduction with 5 μM dimebon and a 80% reduction with 0.05 μM MB + 5 μM dimebon (Fig. 1B–E). The effects were concentration-dependent and statistically significant (Fig. 1E). Thus, 10 μM dimebon caused a 60% reduction and 20 μM dimebon a 70% reduction in the number of TDP-43 inclusions. Similar results were obtained using a second cellular model of TDP-43 proteinopathy (Fig. 2), which expresses a C-terminal fragment (162–414) of TDP-43 as GFP fusion protein [34]. Other anti-histaminergic compounds, including promethazine hydrochloride, diphenhydramine hydrochloride (H1 histamine receptor antagonist) and thioperamide maleate (H3 histamine receptor antagonist) (Sigma–Aldrich, St. Louis, USA), did not affect the number of TDP-43 aggregates (Fig. 3). Similarly, two phenothiazine compounds tested, chlorpromazine hydrochloride and perphenazine (Sigma–Aldrich, St. Louis, USA), which failed to exert any effect on tau aggregation, did not affect the aggregation of TDP-43 (Fig. 3)

3.2. Immunoblot analysis of TDP-43 in cells treated with MB and dimebon

The immunohistochemical results were confirmed by immunoblotting. Cells expressing TDP-43 (ΔNLS&187-192) (data not shown) or the C-terminal fragment (162–414) of TDP-43 (Fig. 4) were sequentially extracted with TS, TX, and Sar, and the supernatants and pellets analyzed by immunoblotting. In cells transfected with the C-terminal fragment (162–414) of TDP-43, phosphorylated C-terminal fragment of TDP-43 was detected in the Sar-insoluble fraction, as reported previously [34] (black arrowhead in Fig 4A). The levels of this band with slower gel mobility were reduced when the cells were treated with MB, dimebon or MB + dimebon (Fig. 4A and B). By contrast, similar levels of endogenous TDP-43 (black arrow in Fig. 4A) and expressed C-terminal fragment of TDP-43 (white arrowhead in Fig. 4A) were detected in TS- and TX-soluble fractions of control cells and of cells treated with MB or dimebon, indicating that these compounds did not affect the amount of TDP-43.

4. Discussion

In this study, we examined the effects of two compounds, MB and dimebon, on the formation of abnormally phosphorylated TDP-43 inclusions using SH-SY5Y cellular models. Both compounds, when used singly or in combination, significantly reduced the number of TDP-43 aggregates. Although its mechanism of action remains to be clarified, it is reasonable to speculate that MB may bind to dimers and oligomers of TDP-43 and thereby inhibit fibril formation, as has previously been demonstrated for the inhibition of Aβ and tau aggregation by MB in vitro [27]. The present findings show, for the first time, that MB can reduce protein aggregation in cells.

In addition, we have identified dimebon as a compound capable of inhibiting the formation of abnormal inclusions of TDP-43. In view of the recent demonstration of its efficacy in a phase II

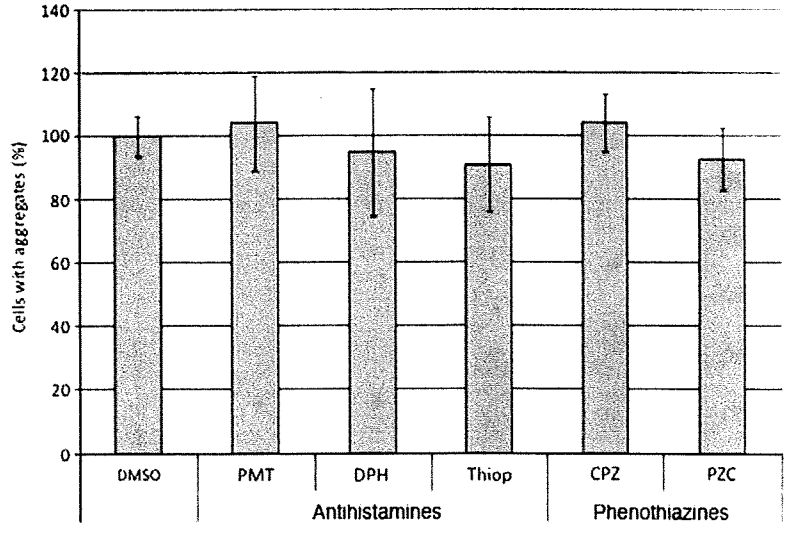

Fig. 3. Immunohistochemical analysis of the effects of three anti-histaminergic compounds, promethazine hydrochloride (PMT), diphenhydramine hydrochloride (DPH) and thioperamide maleate (Thiop), and two phenothiazine compounds, chlorpromazine hydrochloride (CPZ) and perphenazine (PZC) on the aggregation of TDP-43 in SH-SY5Y cells expressing GFP-fused TDP-43 C-terminal fragment (162–414) as GFP fusion protein. Quantitation of cells with TDP-43 aggregates is shown. No reduction in the TDP-43 aggregation was observed with these compounds. Promethazine hydrochloride and phenothiazines were tested at 10 μM and 0.1 μM, respectively, because they were toxic at higher concentrations.

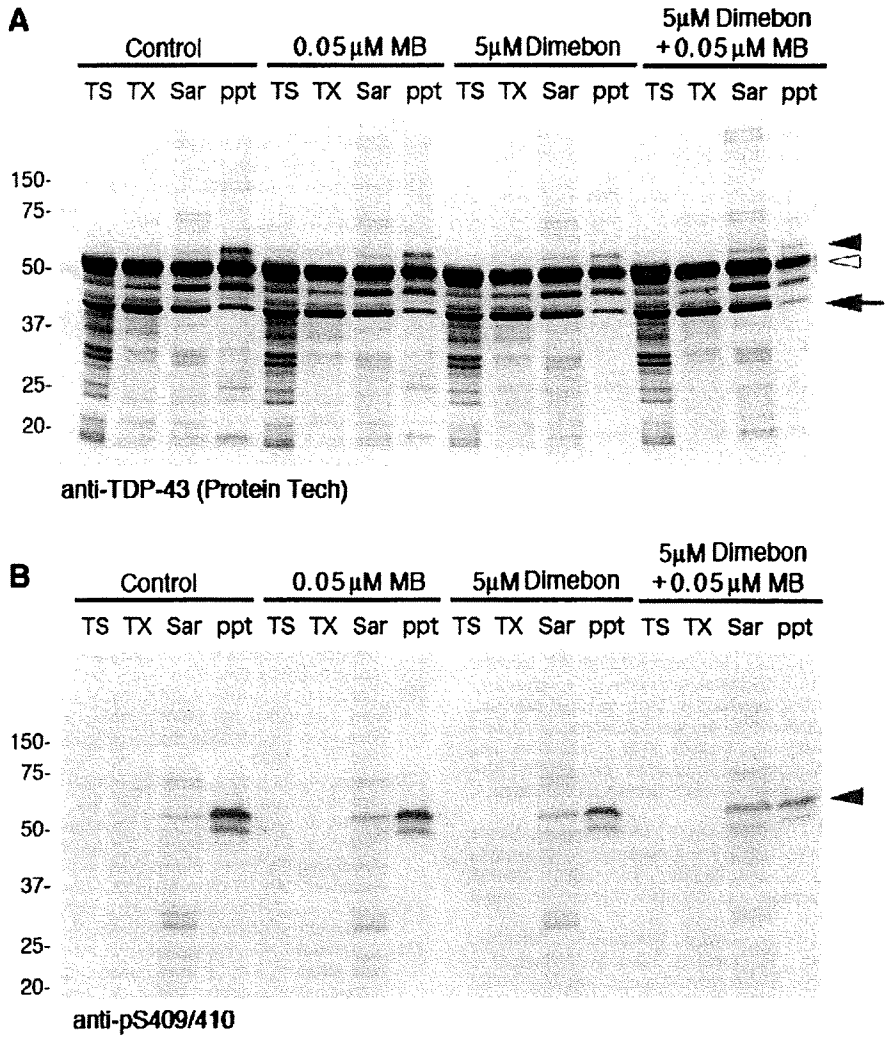

Fig. 4. Immunoblot analysis of the effects of methylene blue (MB) and dimebon on the aggregation of TDP-43 in SH-SY5Y cells expressing GFP-tagged TDP-43 C-terminal fragment (162–414). Tris saline (TS)-soluble material, Triton X-100 (TX)-soluble material, Sarkosyl (Sar)-soluble material and the remaining pellet (ppt) were prepared from control cells and from cells treated with 0.05 μM MB, 5 μM dimebon or 0.05 μM MB + 5 μM dimebon, run on SDS–PAGE and immunoblotted with anti-TDP-43 antibody (A) or anti-pS409/410 antibody (B). Abnormally phosphorylated TDP-43 C-terminal fragment (162–414) with a higher apparent molecular mass than the corresponding non-phosphorylated fragment (white arrowhead) was detected by both antibodies (black arrowheads). Similar levels of the non-phosphorylated GFP-tagged C-terminal fragment of TDP-43 (white arrowhead) and of endogenous TDP-43 (black arrow) were detected with the anti-TDP-43 antibody (A).

clinical trial, dimebon may well become a new drug for the treatment of AD and other neurodegenerative diseases. Although there have been some reports suggesting that dimebon may act as a neuroprotective agent and prevent mitochondrial pore transition in experimental models of AD [36] and Huntington's disease [30], its precise mode of action remains unknown. The present study suggests that dimebon may act by reducing the production or accumulation of abnormal protein aggregates. It remains to be determined whether the effects on TDP-43 aggregation are of a direct or an indirect nature. It will also be interesting to investigate the effects of dimebon in existing [37] and future animal models of TDP-43 proteinopathy. We could not detect a significant effect of dimebon on the in vitro assembly of recombinant human α-synuclein into filaments and on the heparin-induced assembly of recombinant human tau into filaments (data not shown). The recent demonstration that dimebon reduces the number of protein inclusions in a model synucleinopathy [32] suggests that its effects may be indirect.

MB has been used for many years to treat a variety of conditions, including methemoglobinemia [19], septic shock [20] and depression [38]. It has recently been used in a phase II trial of AD [16]. Furthermore, MB has been reported to have activity as an enhancer of mitochondrial activity [24], and a recent study has reported that it delays cellular senescence in cultured human fibroblasts [25]. However, high doses of MB are known to be toxic and to cause the formation of Heinz bodies in erythrocytes in infants [39]. A combination therapy, like the one used here, may therefore be advantageous.

In conclusion, the present results showing a reduction in the number of TDP-43 inclusions following the addition of MB and/or dimebon to transfected SH-SY5Y cells suggest that these compounds may be beneficial for the treatment of ALS and FTLD-U.

Acknowledgements

We thank Dr. Shahin Zibaee for helpful comments on the manuscript. This work was supported by a Grant-in-aid for Scientific Research on Priority Area – Research on Pathomechanisms of Brain Disorders (to M.H., 20023038) from Ministry of Education, Culture, Sports, Science and Technology and grants from Ministry of Health, Labor and Welfare of Japan, and a Russian Foundation for Basic Research Grant (to N.N., 09-04-01412-a).

References

[1] Neumann, M., Sampathu, D.M., Kwong, L.K., Truax, A.C., Micsenyi, M.C., Chou, T.T., Bruce, J., Schuck, T., Grossman, M., Clark, C.M., McCluskey, L.F., Miller, B.L., Masliah, E., Mackenzie, I.R., Feldman, H., Feiden, W., Kretzschmar, H.A., Trojanowski, J.Q. and Lee, V.M. (2006) Ubiquitinated TDP-43 in frontotemporal lobar degeneration and amyotrophic lateral sclerosis. Science 314, 130–133.

[2] Arai, T., Hasegawa, M., Akiyama, H., Ikeda, K., Nonaka, T., Mori, H., Mann, D., Tsuchiya, K., Yoshida, M., Hashizume, Y. and Oda, T. (2006) TDP-43 is a component of ubiquitin-positive tau-negative inclusions in frontotemporal lobar degeneration and amyotrophic lateral sclerosis. Biochem. Biophys. Res. Commun. 351, 602–611.

[3] Davidson, Y., Kelley, T., Mackenzie, I.R., Pickering-Brown, S., Du Plessis, D., Neary, D., Snowden, J.S. and Mann, D.M. (2007) Ubiquitinated pathological lesions in frontotemporal lobar degeneration contain the TAR DNA-binding protein. TDP-43. Acta Neuropathol. 113, 521–533.

[4] Hasegawa, M., Arai, T., Nonaka, T., Kametani, F., Yoshida, M., Hashizume, Y., Beach, T.G., Buratti, E., Baralle, F., Morita, M., Nakano, I., Oda, T., Tsuchiya, K. and Akiyama, H. (2008) Phosphorylated TDP-43 in frontotemporal lobar degeneration and amyotrophic lateral sclerosis. Ann. Neurol. 64, 60–70.

[5] Yokoseki, A., Shiga, A., Tan, C.F., Tagawa, A., Kaneko, H., Koyama, A., Eguchi, H., Tsujino, A., Ikeuchi, T., Kakita, A., Okamoto, K., Nishizawa, M., Takahashi, H. and Onodera, O. (2008) TDP-43 mutation in familial amyotrophic lateral sclerosis. Ann. Neurol. 63, 538–542.

[6] Sreedharan, J., Blair, I.P., Tripathi, V.B., Hu, X., Vance, C., Rogelj, B., Ackerley, S., Durnall, J.C., Williams, K.L., Buratti, E., Baralle, F., de Belleroche, J., Mitchell, J.D., Leigh, P.N., Al-Chalabi, A., Miller, C.C., Nicholson, G. and Shaw, C.E. (2008) TDP-43 mutations in familial and sporadic amyotrophic lateral sclerosis. Science 319, 1668–1672.

[7] Rutherford, N.J., Zhang, Y.J., Baker, M., Gass, J.M., Finch, N.A., Xu, Y.F., Stewart, H., Kelley, B.J., Kuntz, K., Crook, R.J., Sreedharan, J., Vance, C., Sorenson, E., Lippa, C., Bigio, E.H., Geschwind, D.H., Knopman, D.S., Mitsumoto, H., Petersen, R.C., Cashman, N.R., Hutton, M., Shaw, C.E., Boylan, K.B., Boeve, B., Graff-Radford, N.R., Wszolek, Z.K., Caselli, R.J., Dickson, D.W., Mackenzie, I.R., Petrucelli, L. and Rademakers, R. (2008) Novel mutations in TARDBP (TDP-43) in patients with familial amyotrophic lateral sclerosis. PLoS Genet. 4, e1000193.

[8] Kabashi, E., Valdmanis, P.N., Dion, P., Spiegelman, D., McConkey, B.J., Vande Velde, C., Bouchard, J.P., Lacomblez, L., Pochigaeva, K., Salachas, F., Pradat, P.F., Camu, W., Meininger, V., Dupre, N. and Rouleau, G.A. (2008) TARDBP mutations in individuals with sporadic and familial amyotrophic lateral sclerosis. Nat. Genet. 40, 572–574.

[9] Gitcho, M.A., Baloh, R.H., Chakraverty, S., Mayo, K., Norton, J.B., Levitch, D., Hatanpaa, K.J., White 3rd, C.L., Bigio, E.H., Caselli, R., Baker, M., Al-Lozi, M.T., Morris, J.C., Pestronk, A., Rademakers, R., Goate, A.M. and Cairns, N.J. (2008) TDP-43 A315T mutation in familial motor neuron disease. Ann. Neurol. 63, 535–538.

[10] Arai, T., Mackenzie, I.R., Hasegawa, M., Nonoka, T., Niizato, K., Tsuchiya, K., Iritani, S., Onaya, M. and Akiyama, H. (2009) Phosphorylated TDP-43 in Alzheimer's disease and dementia with Lewy bodies. Acta Neuropathol. 117, 125–136.

[11] Hasegawa, M., Arai, T., Akiyama, H., Nonaka, T., Mori, H., Hashimoto, T., Yamazaki, M. and Oyanagi, K. (2007) TDP-43 is deposited in the Guam parkinsonism-dementia complex brains. Brain 130, 1386–1394.

[12] Fujishiro, H., Uchikado, H., Arai, T., Hasegawa, M., Akiyama, H., Yokota, O., Tsuchiya, K., Togo, T., Iseki, E. and Hirayasu, Y. (2009) Accumulation of phosphorylated TDP-43 in brains of patients with argyrophilic grain disease. Acta Neuropathol. 117, 151–158.

[13] Schwab, C., Arai, T., Hasegawa, M., Yu, S. and McGeer, P.L. (2008) Colocalization of transactivation-responsive DNA-binding protein 43 and huntingtin in inclusions of huntington disease. J. Neuropathol. Exp. Neurol. 67, 1159–1165.

[14] Farrer, M.J., Hulihan, M.M., Kachergus, J.M., Dachsel, J.C., Stoessl, A.J., Grantier, L.L., Calne, S., Calne, D.B., Lechevalier, B., Chapon, F., Tsuboi, Y., Yamada, T., Gutmann, L., Elibol, B., Bhatia, K.P., Wider, C., Vilarino-Guell, C., Ross, O.A., Brown, L.A., Castanedes-Casey, M., Dickson, D.W. and Wszolek, Z.K. (2009) DCTN1 mutations in Perry syndrome. Nat. Genet. 41, 163–165.

[15] Schwab, C., Arai, T., Hasegawa, M., Akiyama, H., Yu, S. and McGeer, P.L. (2009) TDP-43 pathology in familial British dementia. Acta Neuropathol., in press, doi:10.1007/s00401-009-0514-3.

[16] Gura, T. (2008) Hope in Alzheimer's fight emerges from unexpected places. Nat. Med. 14, 894.

[17] Doody, R.S., Gavrilova, S.I., Sano, M., Thomas, R.G., Aisen, P.S., Bachurin, S.O., Seely, L. and Hung, D. (2008) Effect of dimebon on cognition, activities of daily living, behaviour, and global function in patients with mild-to-moderate Alzheimer's disease: a randomised, double-blind, placebo-controlled study. Lancet 372, 207–215.

[18] Kristiansen, J.E. (1989) Dyes, antipsychotic drugs, and antimicrobial activity. Fragments of a development, with special reference to the influence of Paul Ehrlich. Dan Med. Bull. 36, 178–185.

[19] Mansouri, A. and Lurie, A.A. (1993) Concise review: methemoglobinemia. Am. J. Hematol. 42, 7–12.

[20] Faber, P., Ronald, A. and Millar, B.W. (2005) Methylthioninium chloride: pharmacology and clinical applications with special emphasis on nitric oxide mediated vasodilatory shock during cardiopulmonary bypass. Anaesthesia 60, 575–587.

[21] Heiberg, I.L., Wegener, G. and Rosenberg, R. (2002) Reduction of cGMP and nitric oxide has antidepressant-like effects in the forced swimming test in rats. Behav. Brain Res. 134, 479–484.

[22] Visarius, T.M., Stucki, J.W. and Lauterburg, B.H. (1997) Stimulation of respiration by methylene blue in rat liver mitochondria. FEBS Lett. 412, 157–160.

[23] Chies, A.B., Custodio, R.C., de Souza, G.L., Correa, F.M. and Pereira, O.C. (2003) Pharmacological evidence that methylene blue inhibits noradrenaline neuronal uptake in the rat vas deferens. Pol. J. Pharmacol. 55, 573–579.

[24] Wrubel, K.M., Riha, P.D., Maldonado, M.A., McCollum, D. and Gonzalez-Lima, F. (2007) The brain metabolic enhancer methylene blue improves discrimination learning in rats. Pharmacol. Biochem. Behav. 86, 712–717.

[25] Atamna, H., Nguyen, A., Schultz, C., Boyle, K., Newberry, J., Kato, H. and Ames, B.N. (2008) Methylene blue delays cellular senescence and enhances key mitochondrial biochemical pathways. FASEB J. 22, 703–712.

[26] Wischik, C.M., Edwards, P.C., Lai, R.Y., Roth, M. and Harrington, C.R. (1996) Selective inhibition of Alzheimer disease-like tau aggregation by phenothiazines. Proc. Natl. Acad. Sci. USA 93, 11213–11218.

[27] Taniguchi, S., Suzuki, N., Masuda, M., Hisanaga, S., Iwatsubo, T., Goedert, M. and Hasegawa, M. (2005) Inhibition of heparin-induced tau filament formation by phenothiazines, polyphenols, and porphyrins. J. Biol. Chem. 280, 7614–7623.

[28] Burns, A. and Jacoby, R. (2008) Dimebon in Alzheimer's disease: old drug for new indication. Lancet 372, 179–180.

[29] Bachurin, S., Bukatina, E., Lermontova, N., Tkachenko, S., Afanasiev, A., Grigoriev, V., Grigorieva, I., Ivanov, Y., Sablin, S. and Zefirov, N. (2001) Antihistamine agent Dimebon as a novel neuroprotector and a cognition enhancer. Ann. NY Acad. Sci. 939, 425–435.

[30] Wu, J., Li, Q. and Bezprozvanny, I. (2008) Evaluation of dimebon in cellular model of Huntington's disease. Mol. Neurodegener. 3, 15.

[31] Lermontova, N.N., Redkozubov, A.E., Shevtsova, E.F., Serkova, T.P., Kireeva, E.G. and Bachurin, S.O. (2001) Dimebon and tacrine inhibit neurotoxic action of beta-amyloid in culture and block L-type Ca(2+) channels. Bull. Exp. Biol. Med. 132, 1079–1083.

[32] Bahurin, S.O., Ustyugov, A.A., Peters, O., Shelkovnikova, T.A., Buchman, V.L. and Ninkina, N.N. (2009). Hindering of proteinopathy-induced neurodegeneration as a new mechanism of action for neuroprotectors and cognition enhancing compounds. Dokl. Biochem. Biophys., in press.

[33] Nonaka, T., Arai, T., Buratti, E., Baralle, F.E., Akiyama, H. and Hasegawa, M. (2009) Phosphorylated and ubiquitinated TDP-43 pathological inclusions in ALS and FTLD-U are recapitulated in SH-SY5Y cells. FEBS Lett. 583, 394–400.

[34] Nonaka, T., Kametani, F., Arai, T., Akiyama, H. and Hasegawa, M. (2009). Truncation and pathogenic mutations facilitate the formation of intracellular aggregates of TDP-43. Hum. Mol. Genet., in press, doi:10.1093/hmg/ddp275.

[35] Johnson, B.S., McCaffery, J.M., Lindquist, S. and Gitler, A.D. (2008) A yeast TDP-43 proteinopathy model: exploring the molecular determinants of TDP-43 aggregation and cellular toxicity. Proc. Natl. Acad. Sci. USA 105, 6439–6444.

[36] Lermontova, N.N., Lukoyanov, N.V., Serkova, T.P., Lukoyanova, E.A. and Bachurin, S.O. (2000) Dimebon improves learning in animals with experimental Alzheimer's disease. Bull. Exp. Biol. Med. 129, 544–546.

[37] Tatom, J.B., Wang, D.B., Dayton, R.D., Skalli, O., Hutton, M.L., Dickson, D.W. and Klein, R.L. (2009) Mimicking aspects of frontotemporal lobar degeneration and Lou Gehrig's disease in rats via TDP-43 overexpression. Mol. Ther. 17, 607–613.

[38] Naylor, G.J., Martin, B., Hopwood, S.E. and Watson, Y. (1986) A two-year double-blind crossover trial of the prophylactic effect of methylene blue in manic-depressive psychosis. Biol. Psychiatr. 21, 915–920.

[39] Sills, M.R. and Zinkham, W.H. (1994) Methylene blue-induced Heinz body hemolytic anemia. Arch Pediatr. Adolesc. Med. 148, 306–310.

The 28-amino acid form of an APLP1-derived Aβ-like peptide is a surrogate marker for Aβ42 production in the central nervous system

Kanta Yanagida[1†], Masayasu Okochi[1,†], Shinji Tagami[1], Taisuke Nakayama[1], Takashi S. Kodama[1], Kouhei Nishitomi[1], Jingwei Jiang[1], Kohji Mori[1], Shin-ichi Tatsumi[1], Tetsuaki Arai[2], Takeshi Ikeuchi[3], Kensaku Kasuga[3], Takahiko Tokuda[4], Masaki Kondo[4], Masaki Ikeda[5], Kentaro Deguchi[6], Hiroaki Kazui[1], Toshihisa Tanaka[1], Takashi Morihara[1], Ryota Hashimoto[1], Takashi Kudo[1], Harald Steiner[7], Christian Haass[7], Kuniaki Tsuchiya[2], Haruhiko Akiyama[2], Ryozo Kuwano[8], Masatoshi Takeda[1]*

Keywords: Alzheimer disease; APLP1 Aβ-like peptides; cerebrospinal fluid; presenilin/γ-secretase

DOI 10.1002/emmm.200900026

Received November 9, 2008
Accepted April 28, 2009

Surrogate markers for the Alzheimer disease (AD)-associated 42-amino acid form of amyloid-β (Aβ42) have been sought because they may aid in the diagnosis of AD and for clarification of disease pathogenesis. Here, we demonstrate that human cerebrospinal fluid (CSF) contains three APLP1-derived Aβ-like peptides (APL1β) that are generated by β- and γ-cleavages at a concentration of ~4.5 nM. These novel peptides, APL1β25, APL1β27 and APL1β28, were not deposited in AD brains. Interestingly, most γ-secretase modulators (GSMs) and familial AD-associated presenilin1 mutants that up-regulate the relative production of Aβ42 cause a parallel increase in the production of APL1β28 in cultured cells. Moreover, in CSF from patients with pathological mutations in *presenilin1* gene, the relative APL1β28 levels are higher than in non-AD controls, while the relative Aβ42 levels are unchanged or lower. Most strikingly, the relative APL1β28 levels are higher in CSF from sporadic AD patients (regardless of whether they are at mild cognitive impairment or AD stage), than those of non-AD controls. Based on these results, we propose the relative level of APL1β28 in the CSF as a candidate surrogate marker for the relative level of Aβ42 production in the brain.

INTRODUCTION

A key feature of the pathology of AD is the accumulation of amyloid-β peptides (Aβ) in senile plaques (Masters et al, 1985; Selkoe, 2001). Aβ is produced *via* endoproteolysis by BACE, which cleaves βAPP at the extracellular domain (Hussain et al, 1999; Sinha et al, 1999; Vassar et al, 1999; Yan et al, 1999), and by the presenilin (PS)–γ-secretase complex (Francis et al, 2002;

(1) Psychiatry, Department of Integrated Medicine, Division of Internal Medicine, Osaka University Graduate School of Medicine, Osaka 565-0871, Japan.
(2) Department of Psychogeriatrics, Tokyo Institute of Psychiatry, Tokyo 156-8585, Japan.
(3) Department of Molecular Neuroscience, Brain Research Institute, Niigata University, Niigata 951-8585, Japan.
(4) Department of Neurology and Gerontology, Kyoto Prefectural University of Medicine, Kyoto 602-8566, Japan.
(5) Department of Neurology, Gunma University School of Medicine, Gunma 371-8511, Japan.
(6) Department of Neurology, Neuroscience, Biophysiological Science, Okayama University Graduate School of Medicine, Dentistry and Pharmacy, Okayama 700-8558, Japan.
(7) Department of Biochemistry, Ludwig-Maximilians-University-Munich, Munich D-80336, Germany.
(8) Department of Molecular genetics, Center for Bioresources, Brain Research Institute, Niigata University, Niigata 951-8585, Japan.
†Equal contribution
*Corresponding author:
Tel: (+81) 6 6879 3053; Fax: (+81) 6 6879 3059;
E-mail: mokochi@psy.med.osaka-u.ac.jp

Yu et al, 2000), which cleaves βAPP in the transmembrane domain (TM) (De Strooper, 2003; Edbauer et al, 2003; Kimberly et al, 2003; Takasugi et al, 2003). To date, no Aβ-like TM-containing peptides from other type-1 TM proteins have been found in brain. However, because *in vitro* studies indicate that Aβ-like peptides derived from Notch-1, CD44, βAPP like protein 1/2 (APLP1/2), alcadein, β-subunits of voltage-gated sodium channels and interleukin-1 receptor II are secreted by cultured cells (Araki et al, 2004; Eggert et al, 2004; Kuhn et al, 2007; Lammich et al, 2002; Okochi et al, 2002, 2006; Wong et al, 2005), we suspected that Aβ-like peptides may exist *in vivo*.

Aβ42 is a major constituent of senile plaques and is thought to induce the pathological process of AD (Selkoe, 2001). Thus the level of Aβ42 production in the brain, especially relative to total Aβ production, is a potential biomarker of the pathological process in AD. However, in patients with AD, the relative ratio of Aβ42 to total Aβ in CSF is lower (Andreasen et al, 1999; Jensen et al, 1999; Motter et al, 1995), probably because Aβ42 in the brain is being cleared more rapidly from the soluble pool by an enhanced rate of deposition/aggregation. To date, surrogate markers for estimating Aβ42 generation in the brain have not been identified. Such surrogate markers might reveal an increased ratio of Aβ42 production and is also associated with the pathology of sporadic AD cases.

In this study, we demonstrate that human CSF contains novel APLP1-derived APL1β species. Our data indicate that brain APL1β28 levels are a surrogate marker for the brain Aβ42 production, as the relative ratio of APL1β28 was up-regulated in CSF samples from patients with a variety of familial AD mutations and sporadic AD.

RESULTS

Identification of novel Aβ-like peptides (APL1β) derived from APLP1 in human CSF

APLP1 and APLP2 are similar to βAPP in the primary sequence and homologous in function (Coulson et al, 2000). To find an *in vivo* Aβ-like peptide, we focused on APLP1 and raised antibodies against the juxtamembrane domain (IQRDELAPAGTGVSRE for OA601 and DELAPAGTGVSRE for OA663). Human CSF was obtained by lumbar puncture from non-demented patients, and proteins were immunoprecipitated using these antibodies or anti-Aβ antibody 4G8. The molecular masses of the precipitated proteins were analysed by matrix-assisted laser desorption/ionization-time of flight (MALDI-TOF) mass spectroscopy (MS). Experiments using OA601 or OA663 detected an identical set of three peptides of 2,329, 2,473and

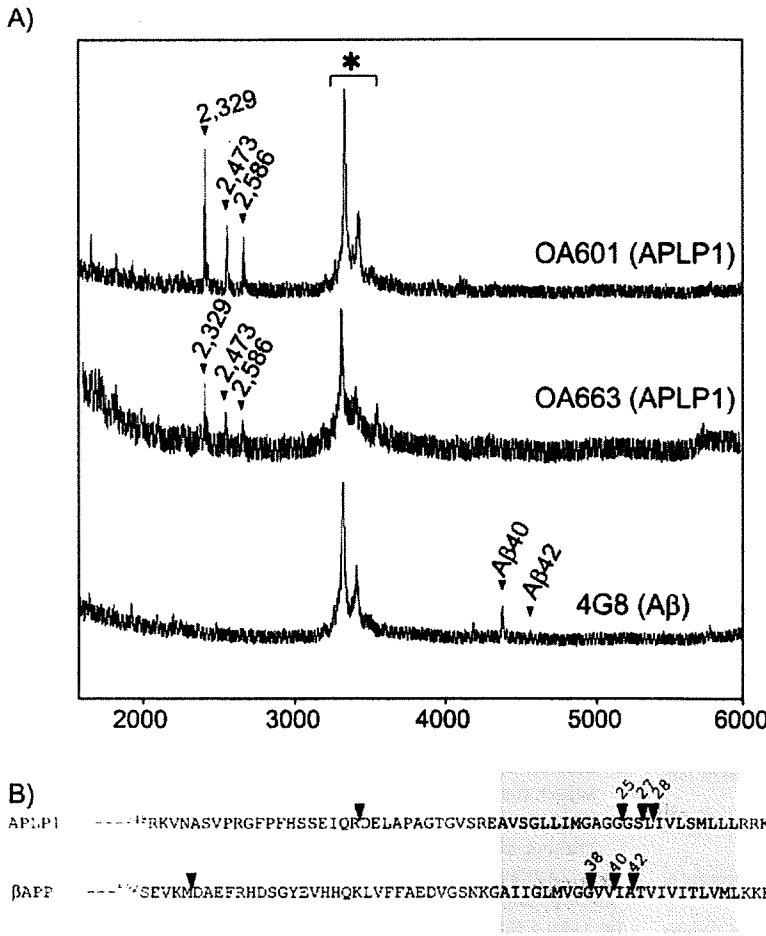

Figure 1. MALDI-TOF MS analysis of APLP1 peptides in human CSF.

A. Determination of the molecular masses of APLP1 peptides in human CSF. Human CSF (300 μl) was immunoprecipitated with the indicated antibodies and analysed by MALDI-TOF MS. Numbers shown on top of the peaks are molecular masses. Asterisks (*) indicate nonspecific peaks.

B. A diagram of the APL1β and Aβ domains in APLP1 and βAPP sequences, respectively. Arrowheads and the grey boxes indicate cleavage sites and the deduced TM, respectively. The numbers above the arrowheads indicate the number of amino acid residues in each fragment.

2,586 Da (Fig 1A). Under the same conditions, the Aβ species were recognized by 4G8 (Fig 1A). On the basis of the molecular weights and the epitopes recognized by the antibodies, we presumed the amino acid sequences of the set of APLP1 peptides. These peptides were named APL1β25 (calculated MW 2,327.2 Da), APL1β27 (calculated MW 2,471.3 Da) and APL1β28 (calculated MW 2,584.3 Da) to reflect the number of amino acid residues in each peptide (see Table S1 of Supporting Information). Finally, the amino acid sequences were determined by using a liquid chromatography-tandem MS (LC/MS/MS) system (see Fig S1 of Supporting Information). Similar to Aβ, the novel brain peptide species derived from APLP1 have a juxtamembrane region at their common N-terminus and a part of the hydrophobic TM at their variable C-termini (Fig 1B).

Sequential endoproteolytic processing by BACE and PS/γ-secretase produces the APL1β species in untransfected SH-SY5Y cells

We suspected that APL1β is generated by a similar process as Aβ. Since naïve SH-SY5Y human neuroblastoma cells were found to secrete the same APL1β species as those found in the human CSF (Fig 2A), degradation of endogenous APLP1 in the cells was then analysed by immunoprecipitation (IP)-MS analysis (Fig 2A). The cells were also radiolabelled with [^{35}S] methionine overnight (Fig 2B) and analysed by IP-autoradiography (Fig 2B; second and fourth panels). Both the IP-MS analysis and the pulse-chase experiments revealed that treatment with a BACE1/2 inhibitor, inhibitor IV, abolishes APL1β secretion. In addition, recombinant BACE1/2 cleaved an APLP1 peptide (Nma-EIQRDELAK(Dnp)-RR-NH2) containing the N-terminus of APL1β as well as a wild-type (wt) βAPP peptide (Nma-EV*KM*DAEFK(Dnp)-RR-NH_2), which contains the N-terminal sequence of Aβ (see Fig S2 of Supporting Information). These results suggest that BACE1/2 can participate in the generation of APL1β which is reminiscent of Aβ generation (Farzan et al, 2000; Hussain et al, 2000).

To determine if PS/γ-secretase is involved in the secretion of APL1β, the cells were treated with the γ-secretase inhibitors DAPT (Fig 2A and B) and L685,458 (Fig 2B). Both compounds abolished APL1β secretion and concomitantly induced intracellular accumulation of APLP1 C-terminal fragment (CTF) stubs, the substrate for γ-cleavage (Fig 2B; third and fourth panels). These results suggest that sequential endoproteolysis by BACE1/2 and PS/γ-secretase mediates APL1β generation.

APL1β and Aβ levels are comparable in human CSF

We next determined how much APL1β is present in the CSF. To do this, an LC/MS/MS system was established to measure the level of each APL1β species. The LC/MS/MS analysis was first performed using synthetic APL1β peptides to select optimal 'daughter (or product)' ions and conditions for quantification (b2, y20 and y21 for APL1β25/28; b2, y21 and y22 for APL1β27; see Fig S3 of Supporting Information). The peak areas of the three daughter ions were measured and the average of three calculated concentrations was defined as the concentration for each APL1β species. Subsequently, various amounts of each synthetic peptide were added to the CSF (50 μl) of patients with

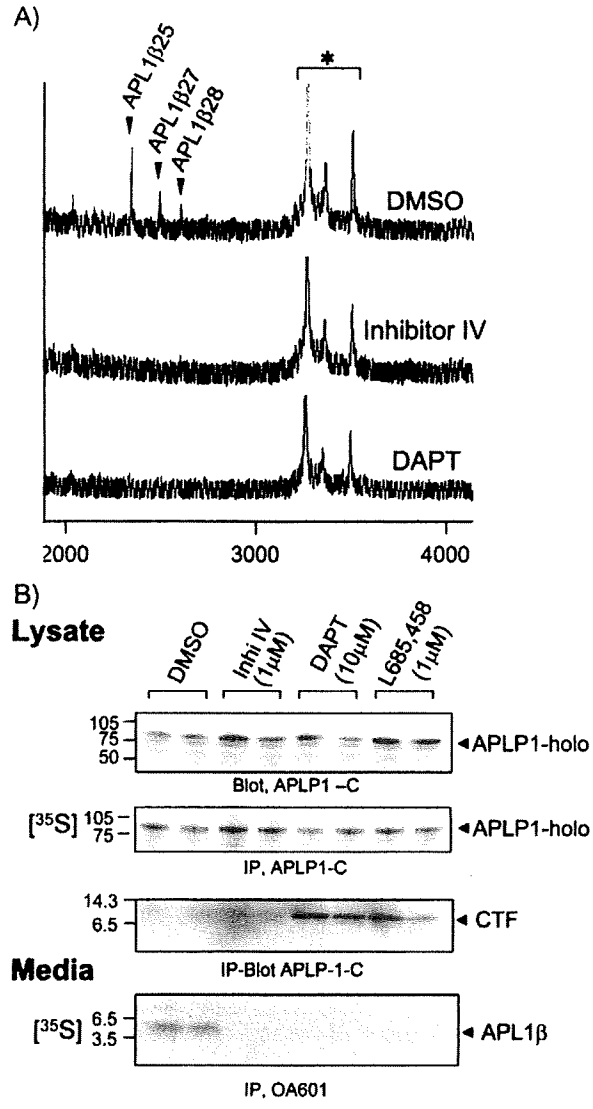

Figure 2. APL1β secretion from naïve SH-SY5Y cells. Inhibition of APL1β secretion from SH-SY5Y cells upon treatment with an inhibitor of BACE1/2 (1 μM inhibitor IV) or PS/γ-secretase (10 μM DAPT or 1 μM L685458).

A. Conditioned media were analysed by IP-MS. Asterisks (*) indicate non-specific peaks.

B. Cells were radiolabelled with [^{35}S] methionine overnight. APL1β (detected via IP-autoradiography) was detected in the conditioned medium (fourth panel). Note that [^{35}S] incorporation in the APL1β bands was abolished by the inhibitors. APLP1 holoprotein (detected *via* direct blotting and IP-autography; first and second panels) and APLP1-CTF stubs (detected *via* IP-blotting; third panel) were detected in the resultant cell lysates. Accumulation of APLP1-CTF stubs upon PS/γ-secretase inhibitor treatment indicates inhibition of degradation of APLP1-CTF stubs, which are the final substrate for APL1β generation following BACE cleavage. Experiments were performed in duplicate (two independent culture dishes).

(Fig 3B) or without AD (Fig 3A). The amounts of synthetic peptide and areas of the resultant daughter ions change in parallel in both the cases. Thus, the levels of each APL1β species in CSF (200 μl) were measured in this system. The APL1β

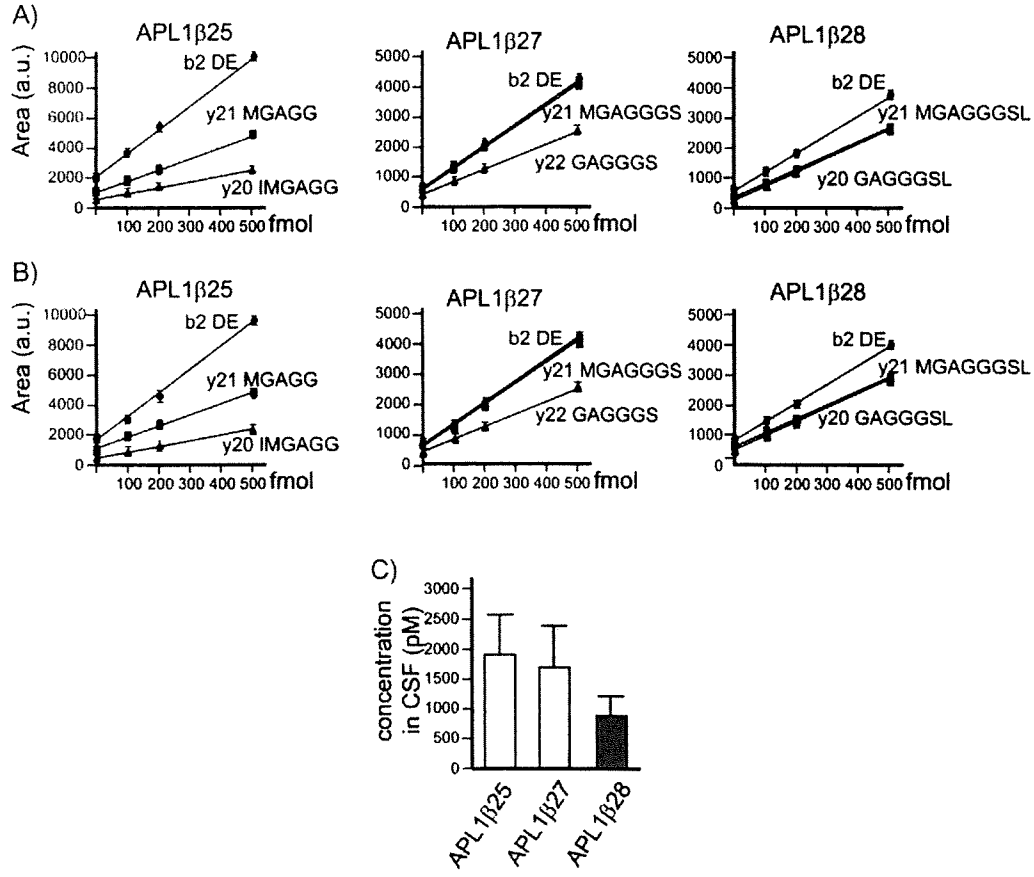

Figure 3. Quantification of APL1β in human CSF by LC/MS/MS.

A. X-axis, levels of the synthetic APL1β added to the CSF; Y-axis, areas of the indicated daughter ions. Note that none of the Y-intercepts is zero. This is due to the presence of APL1β in CSF (C100; non-AD). The experiments were performed three times and values represent mean ± SD.

B. The experiments were repeated using another CSF sample (C114; sporadic AD).

C. Comparison of the level of each APL1β species in human CSF ($n = 17$).

level in CSF from non-demented patients was 4.5 ± 1.7 nM (mean ± S.D. [$n = 17$]; see Table S2 of Supporting Information), and the concentrations of APL1β25, APL1β27 and APL1β28 were 1.9 ± 0.69, 1.7 ± 0.72 and 0.94 ± 0.39 nM, respectively (Fig 3C). Thus, considering the total Aβ level in human CSF (500 pM to 4 nM, depending on the experimental methods for the measurement) (Fukuyama et al, 2000; Ida et al, 1996; Kauwe et al, 2007; Mehta et al, 2000; Southwick et al, 1996; Wiltfang et al, 2007), the results indicate that the level of APL1β in the CSF is similar to or even higher than that of Aβ.

APL1β is not a senile plaque component in AD

We investigated whether APL1β accumulates in senile plaques, as is the case for Aβ. The majority of Aβ in senile plaques is highly insoluble but can be obtained by extraction of the sodium dodecyl sulphate (SDS)-insoluble fraction with 70% formic acid (FA; *i.e.*, FA fraction). Thus, we analysed how much APL1β and Aβ are in the fraction of AD brain samples. The number of Aβ (including smeared bands) levels was calculated by comparison of the densitometric values of the fractions and of synthetic Aβ (see Fig 4A and Fig S4 of Supporting Information). The FA fractions from 2.5 mg of AD brain samples ($n = 2$) contained 0.40–0.80 μg of Aβ (Fig 4A). However, the FA fractions from 65 mg of the same AD brains contained less than 0.1 μg of APL1β (Fig 4B), indicating that the FA fraction of AD brains contains much less APL1β than Aβ (<1%). Immunohistochemical analysis also indicated that neither of the anti-APL1β antisera stain senile plaques in AD temporal lobe tissues (see Fig S5 of Supporting Information). To further characterize the non-aggregative nature of APL1β, we incubated APL1β *in vitro* under Aβ fibril/protofibril formation conditions, and analysed the solution by electron microscopy and size exclusion chromatography (SEC). Even though each APL1β peptide was incubated much longer than Aβ40, no APL1β fibril/protofibril formation could be detected (see Fig 4C–F and Fig S6 of Supporting Information). Collectively, the data indicate a non-amyloidogenic character of APL1β peptides.

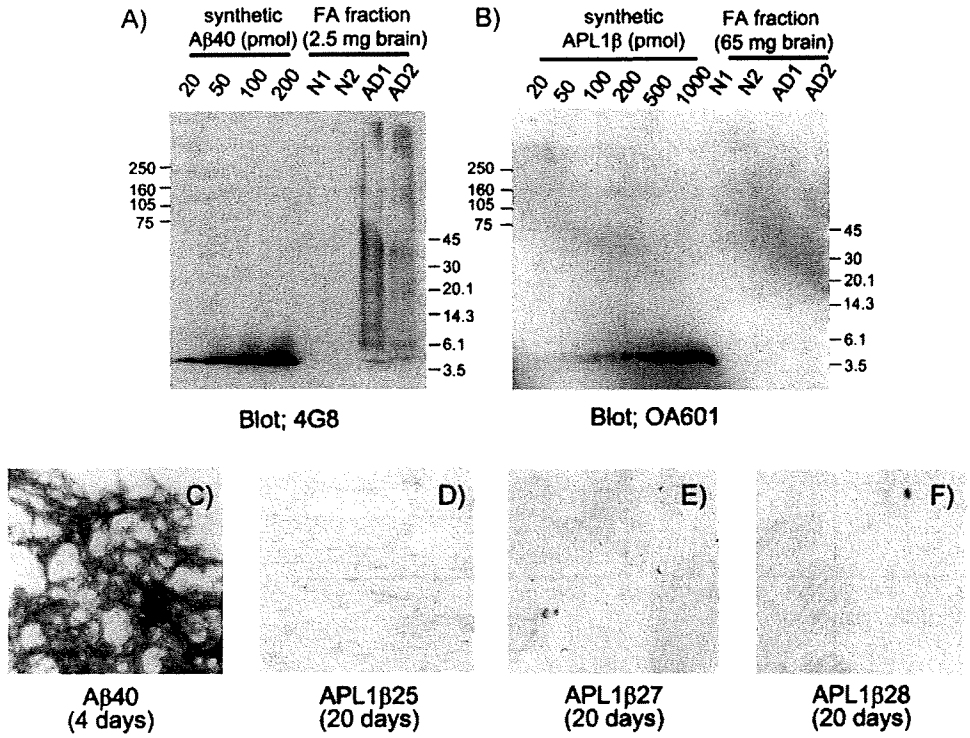

Figure 4. Biochemical and electron microscopic analysis of APL1β.

A. Aβ in the FA fraction of sporadic AD brain samples. The indicated levels of synthetic Aβ40 and Aβ42 mixtures (1:1) and brain FA fractions (extracted from 2.5 mg of non-demented [N1 and N2] or sporadic AD [AD1 and AD2] brain tissue) were subjected to SDS-PAGE and analysed by immunoblotting with monoclonal antibody 4G8. Aβ levels in each FA fraction-containing lane were calculated from the optical densities by comparison with the optical densities of synthetic peptide bands (left four lanes) as a standard.

B. APL1β in the FA fraction. Subsequently, the indicated levels of synthetic APL1β25, APL1β27 and APL1β28 mixtures (1:1:1) and much higher amounts of brain FA fraction (extracted from 65 mg of brain tissue) were immunoblotted with the antibody OA601. Note that OA601 detected a positive signal in the synthetic APL1β mixture but not in the FA fractions.

C–F. Negative staining of Aβ/APL1β peptides incubated *in vitro*. Precipitated fibrils were observed when synthetic Aβ40 was incubated for four days (C). For synthetic APL1β25, 27 and 28 peptides, no fibrils were observed (D–F, respectively).

Some GSMs increase the relative production of APL1β28 in parallel with that of Aβ42 in cell culture

Assuming that the ratio of Aβ42 to total Aβ production in the brain increases in AD, we reasoned that a surrogate marker for Aβ42 production would be a potential biomarker for progression of AD pathology. We studied whether the levels or production of any of the APL1β species might correlate with Aβ42 levels/production. The GSM, S2474, which increases the relative Aβ42 level (Kukar et al, 2005), was added to naïve SH-SY5Y cells, and the levels of secreted APL1β and Aβ species were measured. When the concentration of S2474 in the conditioned medium was increased to 30 μM, the ratio of APL1β28 to total APL1β increased ($R^2 = 0.983$, $t = 29.0$, $p = 1.35 \times 10^{-14}$; Fig 5A). By measuring Aβ40 and Aβ42 generation in conditioned media (Fig 5B), we were able to confirm that increasing the concentration of the compound resulted in an increase in the relative Aβ42 level ($R^2 = 0.9495$, $t = 16.7$, $p = 3.93 \times 10^{-11}$; Fig 5B). Importantly, S2474 increased the ratio of APL1β28 to total APL1β (sum of APL1β25, 27 and 28) in parallel with that of Aβ42 ($R^2 = 0.9578$, $t = 18.4$, $p = 1.02 \times 10^{-11}$; Fig 5C). Similar results were obtained with fenofibrate, another GSM (see Fig S7A of Supporting Information). Thus, the results suggest that APL1β28 generation increases in parallel with Aβ42 generation under these conditions. This is reminiscent of our previous results showing that, among the Nβ species secreted from mouse Notch-1 receptor, some compounds including S2474 and fenofibrate caused parallel changes in the ratios of the longer Nβ25 form to total Nβ and of Aβ42 to total Aβ (Okochi et al, 2006).

Recently, fenofibrate and flubiprofen have been reported to modulate the γ-cleavage by binding to βAPP (Kukar et al, 2008). Although sulindac sulfide (Weggen et al, 2001) and compound-W (Okochi et al, 2006) have been shown to lower the relative Aβ42 level to total Aβ, they did not cause a decrease in the relative APL1β28 level to total APL1β (see Fig S7B–D of Supporting Information). Our results demonstrate that some GSMs, but not all, affect intramembrane proteolysis of human APLP1 as well as βAPP/mNotch-1.

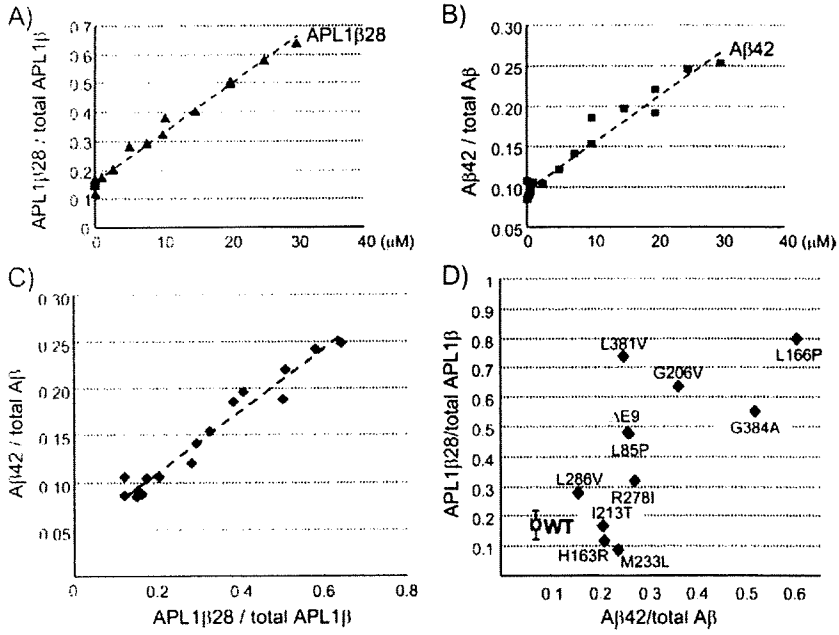

Figure 5. Effects of GSM and PS1 familial AD mutations on the relative ratio of APL1β28 production in cell culture. The levels of APL1β and Aβ in conditioned medium were determined using IP-LC/MS/MS or the sandwich ELISA system, respectively.

A. Changes in relative APL1β28 levels after the addition of the indicated concentrations of S2474.

B. Changes in relative Aβ42 levels after the S2474 addition. Note that the generation of Aβ42 increased as the dose of S2474 was increased.

C. Relationship between the relative levels of APL1β28 *versus* Aβ42 upon S2474 treatment.

D. Relationship between the relative levels of APL1β28 *versus* Aβ42 secreted from K293 cells stably expressing the indicated mutant forms of PS1 FAD. The values indicate means of two independent experiments without SEM.

Several FAD-associated presinilin 1 (PS1) mutants up-regulate the relative production of APL1β28 as well as that of Aβ42 in cell culture

We also examined whether FAD mutants in PS1 can cause, in addition to their effect on Aβ42, an increase in the ratio of APL1β28 to total APL1β. Previous studies using PS1 mutant-transgenic mice report that the magnitude of the increase in the relative Aβ42 level in cultured cells reflect the magnitude of increase in the brain (Borchelt et al, 1996; Citron et al, 1997). We chose the mutants PS1 L85P, H163R, L166P, G206V, I213T, M233L, R278I, L286V, L381V, G384A and ΔE9. We prepared human embryonic kidney 293 (HEK293) cells stably expressing βAPP Swedish (sw), wt APLP1, and each of the selected PS1 FAD mutant forms. In the stable cell lines, endogenous PS proteins in PS/γ-secretase complex were successfully displaced by the exogenous mutant form (see Fig S8 of Supporting Information). Analysis of conditioned media revealed that many of the PS1 mutants increase the relative level of APL1β28 and Aβ42 in parallel (Fig 5D).

However, three of the mutant forms, PS1 H163R, I213T and M233L, were exceptions and had very minor or no effects on the rate of increase in relative APL1β28 production (wt PS background, mean ± SD = 0.163 ± 0.031) (Fig 5D). This is reminiscent of our previous finding that FAD-associated PS1 C92S does not increase the relative amount of Nβ25 generated from Notch1 (Okochi et al, 2006). Thus, there may be PS1 mutant forms that affect the interaction between βAPP and PS/γ-secretase but not the interaction between APLP1 and PS/γ-secretase.

In CSF from patients and in cultured cells, some PS1 FAD mutations cause a parallel increase in the ratio of APL1β28 to total APL1β

As APL1β28 is not detected in insoluble AD brain fractions (Fig. 4), we examined whether the relative APL1β28 level in CSF reflects the relative production of Aβ42 in the brain. We prepared CSF from patients bearing PS1 FAD mutants (PS1 L85P, H163R, G206V, M233L, L286V and L381V) (Table 1) and from non-demented patients (see Table S2 of Supporting Information), and measured the level of each APL1β and Aβ species in the samples (Fig. 6).

Table 1. Clinical information of the familial AD patients in this study

Mutation	Diagnosis	Age of onset (Year)	Age of CSF collection (Year)	Symptoms
PS1 L85P	Early onset AD with spastic paraplegia (variant type AD)	26	27	MMSE23/30
PS1 H163R	Early onset AD with parkinsonism	41	48	MMSE3/30
PS1 G206V	Early onset AD with psychosis	37	38	MMSE10/30
PS1 M233L-1	Early onset AD with parkinsonism	41	48	MMSE2/30
PS1 M233L-2	Early onset AD with spastic paraplegia	37	53	MMSE0/30, bed-ridden
PS1 L286V	Early onset AD	40	47	MMSE22/30, CDR1
PS1 G381V	Early onset AD with spastic paraplegia (variant type AD)	29	57	MMSE0/30, bed-ridden

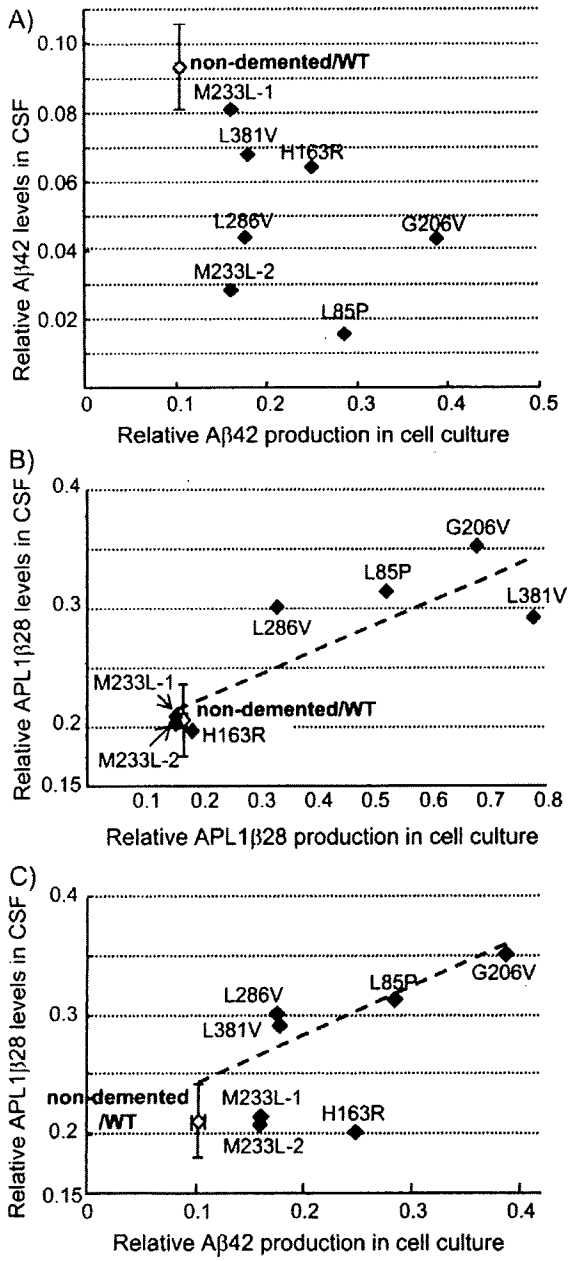

Figure 6. Relative APL1β28 levels in CSF of PS1 FAD patients.

A. Relationship between the relative ratio of Aβ42 level to total Aβ level in the CSF (for the non-demented patients with wt PS1 [$n = 17$] or patients with the indicated PS1 FAD mutations) and the relative ratio of Aβ42 production to total Aβ production in cell culture (K293 cells stably expressing wt PS1 or the indicated PS1 FAD mutants). For non-demented patients, the value is a mean, and the error bar represents the SD.

B. Relationship between the relative ratio of APL1β28 level to total APL1β level in the CSF and the relative ratio of APL1β28 production to total APL1β production in cell culture. Patients M233L-1 and M233L-2 are brothers.

C. Relationship between the relative ratio of APL1β28 level to total APL1β level in the CSF and the relative ratio of Aβ42 production to total Aβ production in cell culture.

We first calculated the relative Aβ42 levels in the CSF and then compared the values with those secreted from wt PS or the PS mutant-expressing cells (Fig 6A). As expected, although the relative levels of Aβ42 secreted from the mutant cells were elevated (wt PS background, mean ± SD = 0.104 ± 0.004), the relative levels of Aβ42 in the CSF were unchanged or decreased (non-demented patients, mean ± SD = 0.093 ± 0.010) (Fig 6A). Thus, it seems that the relative Aβ42 levels in CSF do not correspond to the relative generation of Aβ42 in FAD brains.

We, next, performed a similar study with APL1β (Fig 6B). More specifically, the relative APL1β28 levels in mutant CSF were compared with the levels secreted from mutant cells. PS1 L85P, L286V, G206V and L381V mutants were found to up-regulate the relative APL1β28 level in conditioned medium (Fig 5D). In contrast to what was found for Aβ42, the relative APL1β28 level is, indeed, up-regulated in CSF of the FAD patients bearing these mutants (non-demented patients, mean ± SD = 0.208 ± 0.030) (Fig 6B). However, in CSF of patients bearing the mutations PS1 H163R and M233L, which do not increase the relative APL1β28 level in conditioned medium (Fig 5D), the relative level of APL1β28 is not up-regulated (Fig 6B). These results suggest that, as for the PS1 FAD mutations, the relative APL1β28 levels in CSF correlate with the relative generation of APL1β28 in the brain ($R^2 = 0.74$, $t = 4.10$, $p = 0.006$; Fig 6B). Collectively, we found that PS1 FAD mutations that increase the relative levels of Aβ42 and APL1β28 in cell culture, also elevate the relative CSF levels of APL1β28 but not Aβ42 (Fig 6C). Thus, APL1β28 is a potential surrogate marker for Aβ42. That is the relative level of APL1β28 in CSF correlated with the relative generation of Aβ42 in the brain ($R^2 = 0.79$, $t = 3.31$, $p = 0.04$; Fig 6C).

Even at the mild cognitive impairment (MCI) stage, the relative level of APL1β28 in the CSF of sporadic AD patients is higher than that of non-AD controls

Given that APL1β28 may be a non-aggregating surrogate marker for Aβ42, we examined whether the relative ratio of APL1β28 in the CSF changes in sporadic AD patients. We measured APL1β and Aβ species in CSF of patients with sporadic AD (M = 43) including those who were at the MCI stage ($n = 9$) and in demented patients without AD ($n = 35$) as well as in non-demented individuals ($n = 17$) (Supplementary Table 2). The relative ratios of APL1β28 are plotted against those of Aβ42 in Fig 7A. As clearly shown, results for many of the sporadic AD patients were located in the lower-right part (a location where APL1β28 ratio is high and Aβ42 ratio is low) of the plot. Statistically, even when the patients were at the MCI stage (mean ± SEM = 0.248 ± 0.003), the relative APL1β28 level in the CSF of sporadic AD patients (0.263 ± 0.001) was higher than that of non-demented (0.208 ± 0.002) or non-AD patients (0.212 ± 0.002) with significant differences between non-demented and sporadic AD patients ($p < 0.0001$), non-demented and MCI-stage patients ($p < 0.01$), non-AD and sporadic AD patients ($p < 0.001$), and non-AD and MCI-stage patients ($p < 0.05$), according to the Kruskal–Wallis and Wilcoxon–Mann–Whitney tests (Fig 7B). In addition, we also observed the lowered tendency of the relative Aβ42 level in the CSF of

